MONITORING THE AVAILABILITY AND QUALITY OF INCOMING GTS OBSERVATIONS AT ECMWF

F. Delsol

European Centre for Medium Range Weather Forecasts

1. INTRODUCTION

During the past two years, ECMWF has enhanced the monitoring of the global observational data set available via the Global Telecommunication System and used as the basis of its operational forecasting activity.

This increasing effort in monitoring has three main justifications:

First: Analysis errors propagate and spread during the forecast so that a good global data coverage is essential for medium range forecasting.

Second: the horizontal resolution of the analysis is increasing, therefore the quality control of the data based on the horizontal redundancy becomes more difficult and a priori quality control is needed to exclude bad observations.

Third: the quality of the first guess has steadily improved, so that the negative impact of bad observation is more damaging and occurs with smaller errors in the observations.

This paper presents the different tools which have been developed in the ECMWF operational system as described in Lönnberg and Shaw (1983) and Louis (1984a,b) Operational applications are presented with examples of the day to day real time data monitoring, as well as examples of the post mortem data monitoring.

2. REAL TIME MONITORING

Real time monitoring involves the day to day survey of the availability and the quality of the observations as received via the GTS at ECMWF.

2.1 Real time monitoring of the availability of the observations

The purpose of this part of the monitoring is to check in real time that all the expected observations have been received and properly decoded.

First the raw bulletins which failed the decoding are accumulated and corrected manually before being presented to the decoding procedure once again (Fig. 1). After decoding, data coverage maps of each observation types for the 4 analysis cycles (00z, 06z, 12z, 18z) are examined in order to ensure full reception of the data (Fig. 2). The total number of observations from the last 7 days (Fig. 3) for both hemispheres also provides also a good warning of possible deficiences. Any lack of data leads to the investigation of possible transmission or decoding problems.

2.2 Real time monitoring of the quality of the observations

The observations successfully decoded are presented to the data assimilation process which provides the global analysis, used as the initial state of the atmosphere for the forecast model. For each of the 4 assimilation cycles (Fig. 4), a 6h forecast from a previous analysis is used as a first guess. The analysis is a modification of this first guess by the observations using a three-dimensional multivariate optimum interpolation technique.

The quality of the first guess is already very good, therefore it is essential to ensure that the data do not degrade the first guess but do correct its errors. This is performed by several quality control mechanisms at different stages of the assimilation and bad observations are eventually rejected. The quality control checks consist of:

- Comparison to climatology
- Internal consistency, hydrostatic check
- Comparison to first guess
- Comparison to a local analysis excluding the observation to be checked

Figure 5 shows a map of rejected data; each symbol corresponds to a different observation. Any anomaly such as an excessive number of rejections, for example the group of buoys (Dribus) and satellite soundings (Satem)shown in Fig. 5, leads to further investigations; systematic plots are produced of all observations together with the analysis and the first guess.

The next step is to look at the impact of the observations in the assimilation as represented by the analysis increments, i.e. the difference between analysis and firstguess. Figure 6 shows an example of a 200 mb increment chart for the height and wind. Excessive values may indicate either a data problem or a first guess problem For example in Fig. 6, the large wind and height increments were caused by a mislocated aircraft; Fig. 7 shows the track used in the original analysis and to correct track. The corresponding ASDAR processing centre was contacted and the problem rapidly cured.

Difference maps between the ECMWF analysis and analyses from other centres available on the GTS (NMC, Tokyo, Bracknell, Paris, Offenbach) are produced every day (mean sea level pressure and 500 mb height) and systematic differences are investigated. Figs. 8 and 9 show an example where the differences could be explained by the much longer cut-off time of the data used at ECMWF.

3. POST MORTEM MONITORING

The day to day monitoring is essential in order to react quickly to problems, but does not provide a good understanding of the systematic deficiencies in the availability and the quality of the data. An accumulation of results with statistics over a long period of time, typically one month, three months or one year, is needed.

3.1 Post mortem monitoring of the availability of the data

The quality of the medium range weather forecast is dependent on good global distribution of the observations. It has been shown for instance that an analysis error over the north Pacific propagates eastwards during the forecast and reaches Europe after 5 days. (cf A. Hollingsworth et al., 1985)

A good way to investigate the spatial distibution of the data is to plot all the observations used for one analysis time during one month. Figs. 10 and 11 show an example for aircraft reports and ship reports at 12Z; all observations received up to 24 h after observation time have been accumulated. The lack of observations in the southern hemisphere and the very poor coverage of aircraft reports over continents are very clear. Fig. 12 shows for 12Z the ship observations received too late to be used, after 2015Z, during one month. Note in particular that many reports corresponding to night time observation in the Australian area are systematically delayed during transmission.

The rate of arrival of observations is essential information required to define an adequate cut-off time of the data. Figures 13 and 14 show examples for rawinsonde and ship observations.

3.2 Post mortem monitoring of the quality of the data

The main technique used at ECMWF for monitoring the quality of the observations received on the GTS is the comparison of the observations with the 6 hours forecast used as a first guess, and the analysis (initialised and uninitialised). The operational assimilation system provides every day for 00z and 12z analysis the differences between each available observation and the interpolated value at the observation point of the analysis and first guess for the 00Z and 12Z analyses. These values are systematically archived on tape month by month. This represents one tape per month for one analysis time, Satem data excluded. A large quantity of very valuable information on the quality of observations and first guess can be derived from this archive. (Hollingsworth et al, 1985/b).

3.2.1 Ground based observation

For individual stations or ships, the bias and the standard deviation of the differences from the first guess and analysis can be computed according to their call sign. Different presentations of the results are possible and typical examples are shown in Figs. 15 to 18 for rawinsonde observations. Fig. 15 shows the geographical distribution of the standard deviation of the height departure in metres at 500 mb, while Fig. 16 shows the wind bias at 700 mb. Such maps provide a powerful tool for detecting suspected rawinsonde stations by comparison with surrounding stations.

The vertical structure of the bias and standard deviation can give further indications about the behaviour of the observations at a particular station (Fig. 17), but the final evaluation of the quality of the observations is based on the complete time series of the observation during the month. See example Fig. 18.

Another way of monitoring observations is to examine the mean change made by the analysis. Fig. 19 gives the March 1984 monthly mean difference between the analysed 200 mb wind field and first guess; this clearly illustrates the excessive north increment in the South Atlantic due to Gough Island rawinsonde station. Fig. 20 shows the March 1984 time series of observed minus first guess wind at Gough Island with a systematic north component.

The data producer was contacted after a local enquiry and found an error in the wind direction reference. The bias disappeared the following month. With regard to ship reports, bias and root mean square errors can be computed according to their call sign. This provides a systematic way to survey ship data and thus produce a blacklist of the kind shown in Fig. 21.

3.2.2 Satellite observations

Similar techniques can be extended to the monitoring of satellite information such as SATOB cloud motion vectors derived from geostationary satellites, or temperature soundings from polar orbiting satellites. In order to have a sufficient number of observations, all observations inside a 5° x 5° box are used to compute the bias and standard deviation of the differences between the observation and the first guess for a period of one month. Figs. 22 to 25 present examples of results for Meteosat. The interpretation of such statistics has to take into account the first guess error. To overcome this problem we derive the same statistics for other observation types and then compare them. Figs. 26 to 29 show the bias and standard deviation of the wind at the same level during the same period for aircraft wind reports and rawinsonde wind reports. In this example, an underestimation by the satellite observations of the wind speed in the jet over North Africa is indicated by aircraft and rawinsonde observation. Full agreement between independent observing systems would have suggested an error in the first guess. This method is a very powerful tool to study both the spatial distribution of the observation error and the first guess error. The same technique can be applied to polar orbiting satellite soundings.

References

Chambers, J., Basic functional design of ECMWF's Meteorological Operational System. ECMWF Meteorological Bulletin M1.

Hollingsworth, A., A. Lorenc, M.S. Tracton, K. Arpe, G. Cats, S. Uppala, and P. Kallberg, 1985a: The response of numerical weather prediction systems to FGGE Level III-b data, Part I: Analyses. Quart.Jour.Roy.Met.Soc., 111, 1-66.

Hollingsworth, A., D.B. Shaw, P. Lönnberg, L. Illari, K. Arpe, A.J. Simmons, 1985/b "Monitoring of Observation and Analysis Qulaity by a Data Assimilation System", in Proceedings of ECMWF/WMO Seminar on Data Assimilation Systems and Observing System Experiment with particular emphasis on FGGE. pp.393-441.

Hooper, A.H., 1975: Upper-air sounding studies, Vol. I: Studies on Radiosonde performance. WMO Tech. Note. 140.

Hubert, L.F., 1979: Wind derivation from geostationary satellites. In: Quantitative meteorological data from satellites (J.S. Winston, ed.). WMO Technical Note No. 166, WMO-No. 531, 33-59.

JPS 1981-1982 FGGE Operations Report. Vol. 1-12. ICSU/WMO, Geneva.

Johnson, D.S., 1985: Meteorological parameters derived from space-based observing systems - FGGE and after. ECMWF Seminar on Data Assimilation Systems and Observing System Experiments with Particular Emphasis on FGGE, 3-7 September 1984, Reading, U.K., 47-108.

Kallberg, P., S. Uppala, N. Gustafsson and J. Pailleux, 1982: The impact of cloud track wind data on global analyses and medium range forecasts. ECMWF Tech. Rep. No. 34, 54pp.

Lönnberg, P. and D. Shaw, 1983: ECMWF Data Assimilation Scientific Documentation. ECMWF Research Manual 1.

Louis, J-F., 1984: Guide to the ECMWF Forecasting system. ECMWF Meteorological Bulletin M2.

Morgan, J., and D.E. Chapman, 1983: Error characterising of atmospheric wind measurements. ESA Report of the 4th Meteosat scientific meeting, 1983.

Shaw, D., P. Lönnberg, and A. Hollingsworth, 1984: The 1984 revision of the ECMWF analysis system. ECMWF Tech. Rep. No. 92, 69pp.

Suchman, D., and D.W. Martin, 1976: Wind sets from SMS images: an assessment of quality for GATE. J. Appl. Met., 15, 1265-1278.

Whitney, L.F., Jr., 1983: International comparison of satellite winds - update. Adv. in Space Res., 2(6), 73-77.

```
0B49660016    85/06/21    00.29.09.
 037 18300
 SMVX1 EESA 210000
 BBXX
 DBFM   21003 99584 70070
 42/98 80909 10127 20094 40060 57018
 22262 00117 ICE TEMP UUAA 7023/ 99585 50064 18186 99007 13243 1101
 0 00060 13047 85401 02823 70941 06967 50551 18348 UUBB 7023/ 99585
 50064 18186 00007 13243 11962 10857 22858 03023 33718 06714 44699
 06974 55514 18132 66497 18350 21212 00007 11010 41414 00942=
```

```
CORRECTED    85/06/21    00.29.09.
 037 18300
 SMVX1 EESA 210000
 BBXX
 DBFM   21003 99584 70070 42/98 80909 10127 20094 40060 57028
 22262 00117=
```

```
CORRECTED    85/06/21    00.29.09.
 037 18300
 USVX1 EESA 210000
 UUAA   7023/ 99585 70064 18186 99007 13243 11010 00060
 13047 85401 02823 70941 06967 50551 18348=
```

```
CORRECTED    85/06/21    00.29.09.
 037 18300
 UKVX1 EESA 210000
 UUBB   7023/ 99585 70064 18186 00007 13243 11962 10857 22858
 03023 33718 06714 44699 06974 55514 18132 66497 18350 21212
 00007 11010 41414 00942=
```

Fig. 1 Example of manual correction of bulletin

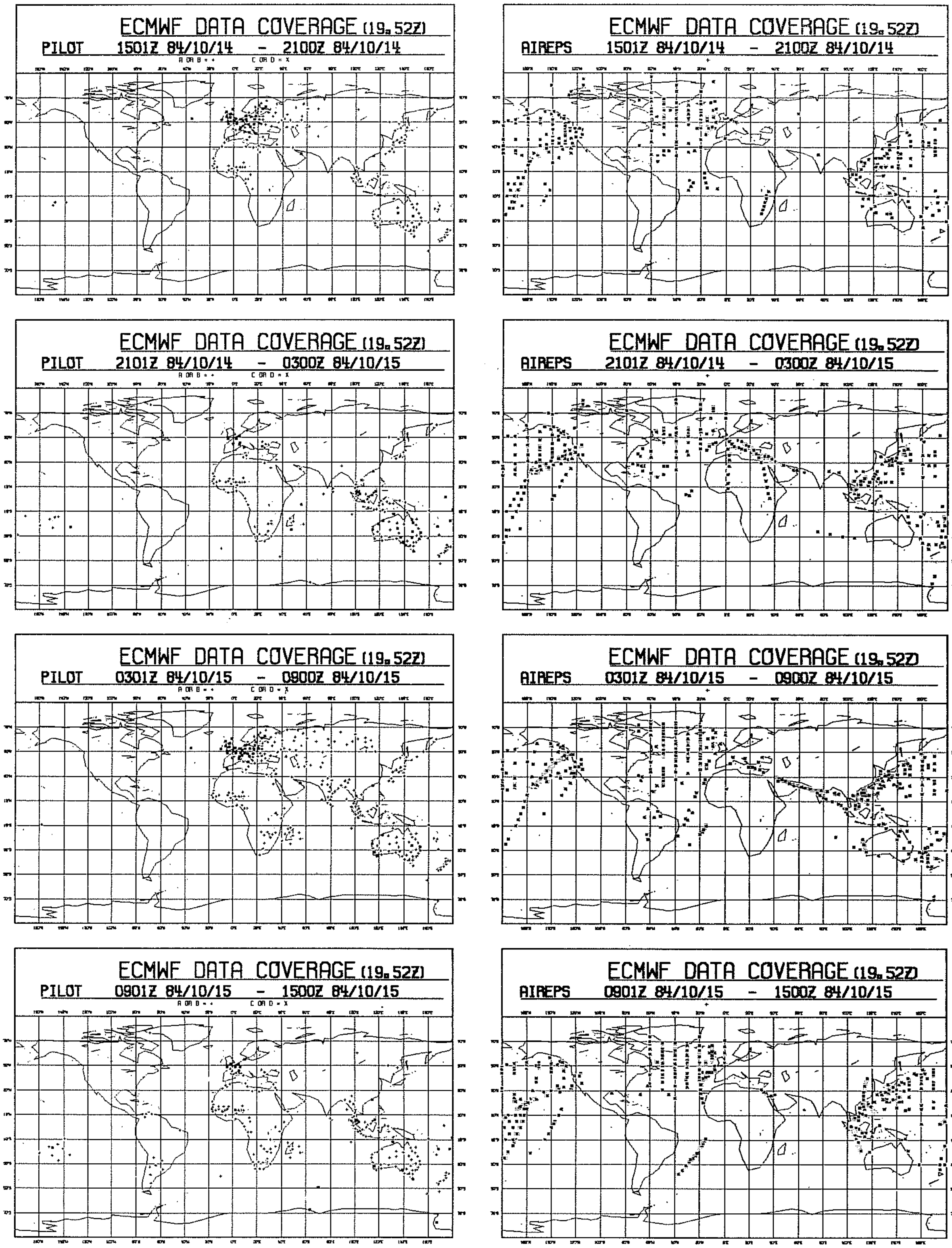

Fig. 2 Data coverage

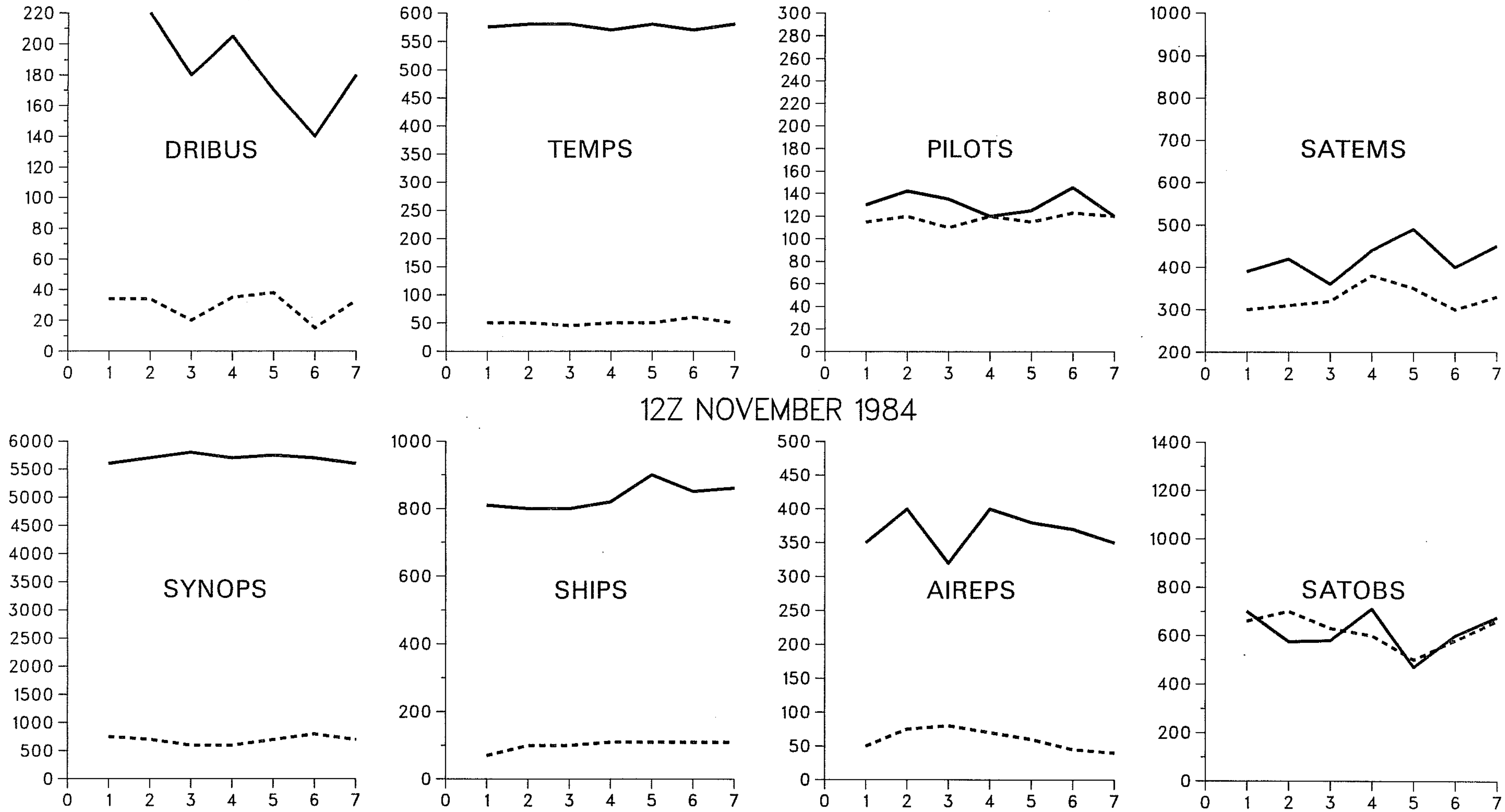

Fig. 3: Number of reports received during the past 7 days NH (solid line) and SH (dashed line) by observation type.

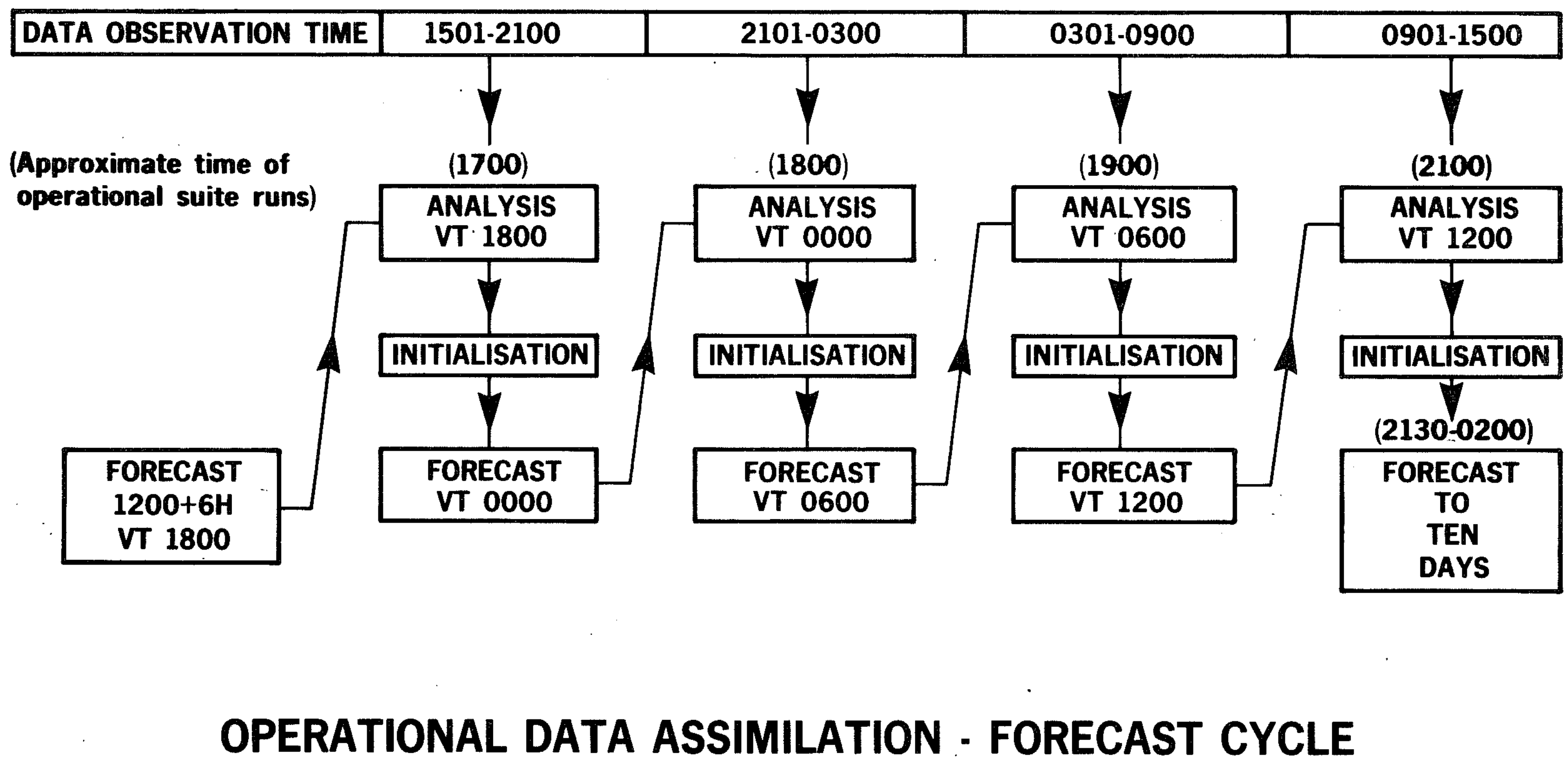

Fig. 4 ECMWF data assimilation cycle

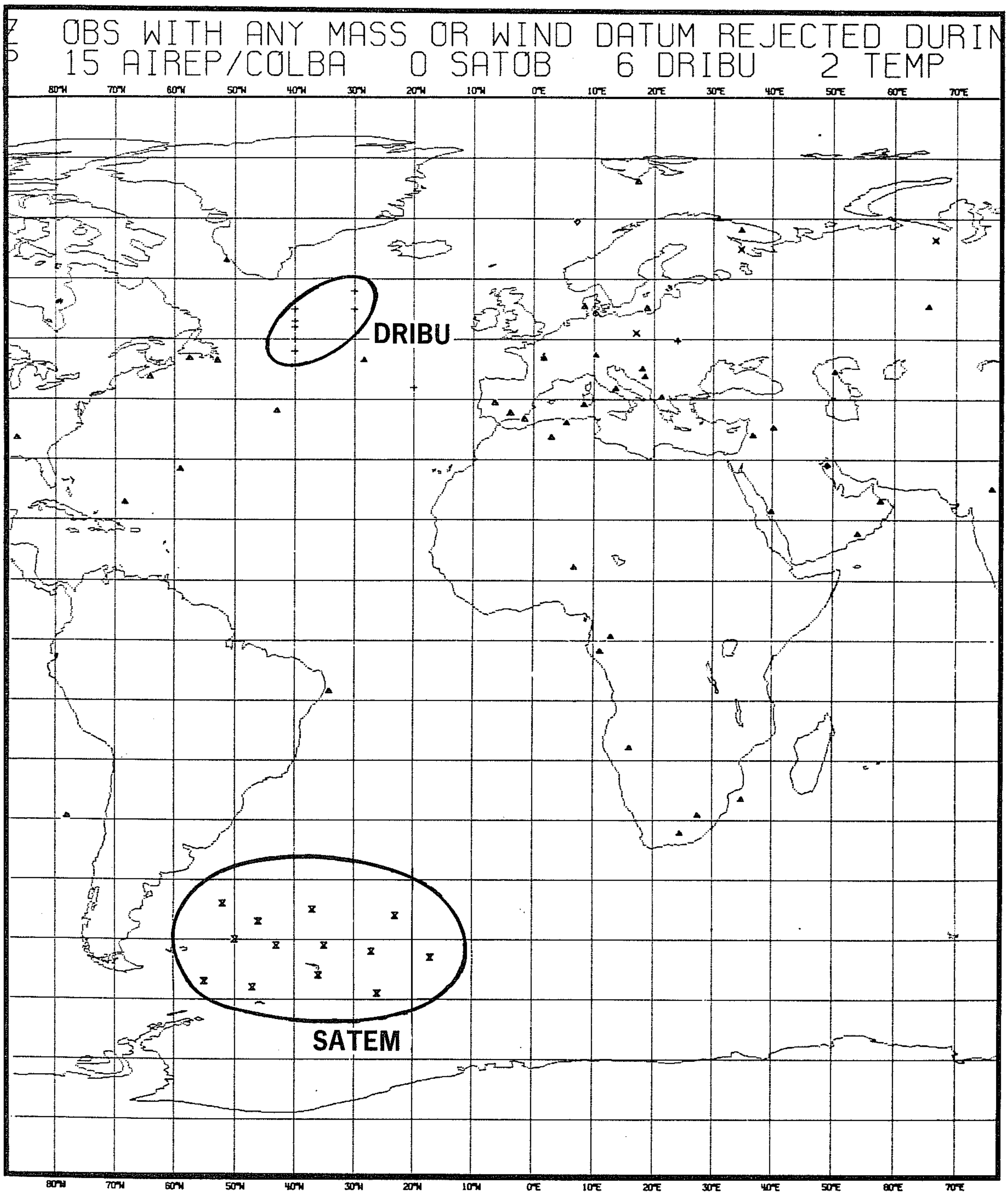

Fig. 5 Data rejection map

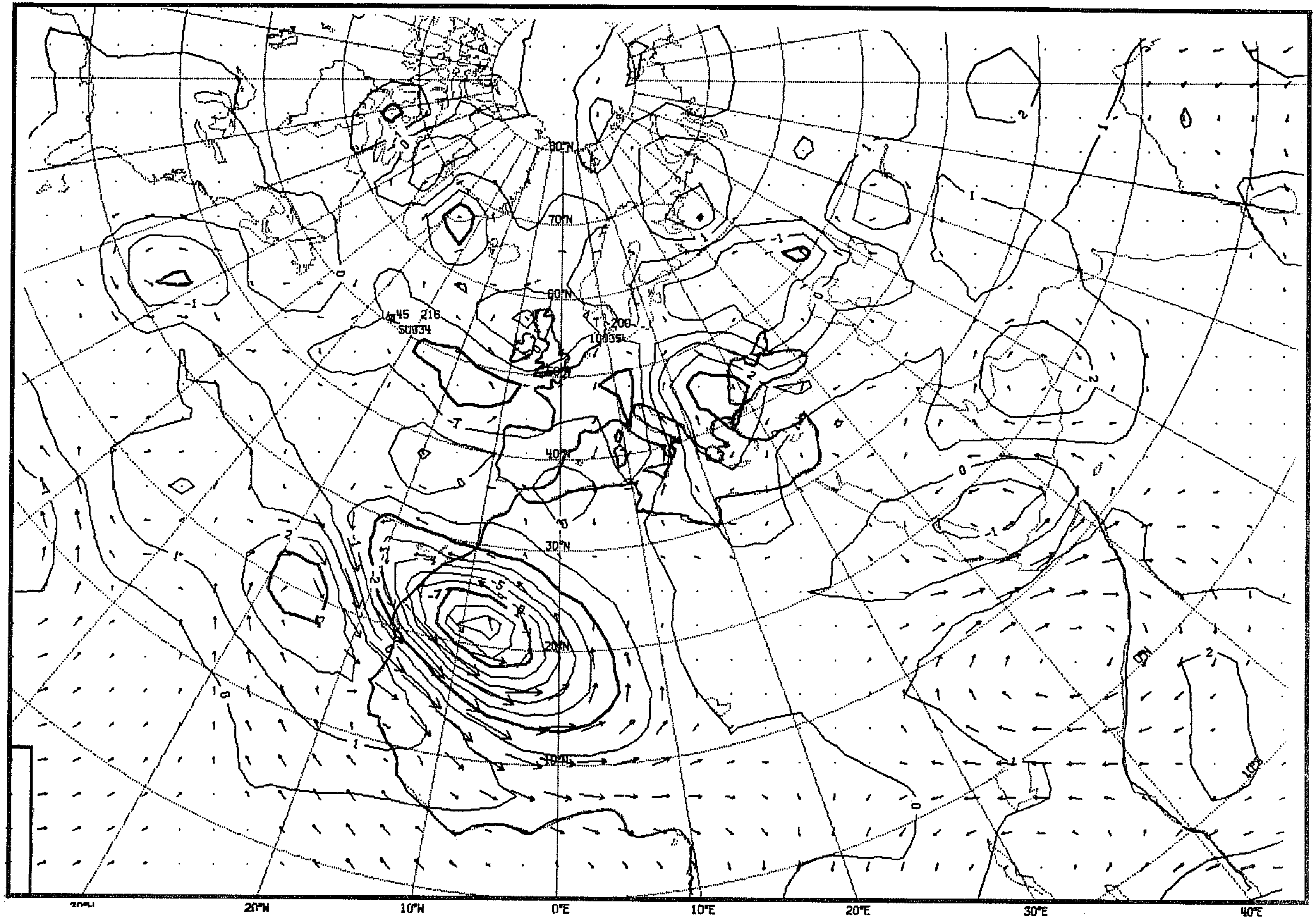

Fig. 6 200 mb height and wind increment chart

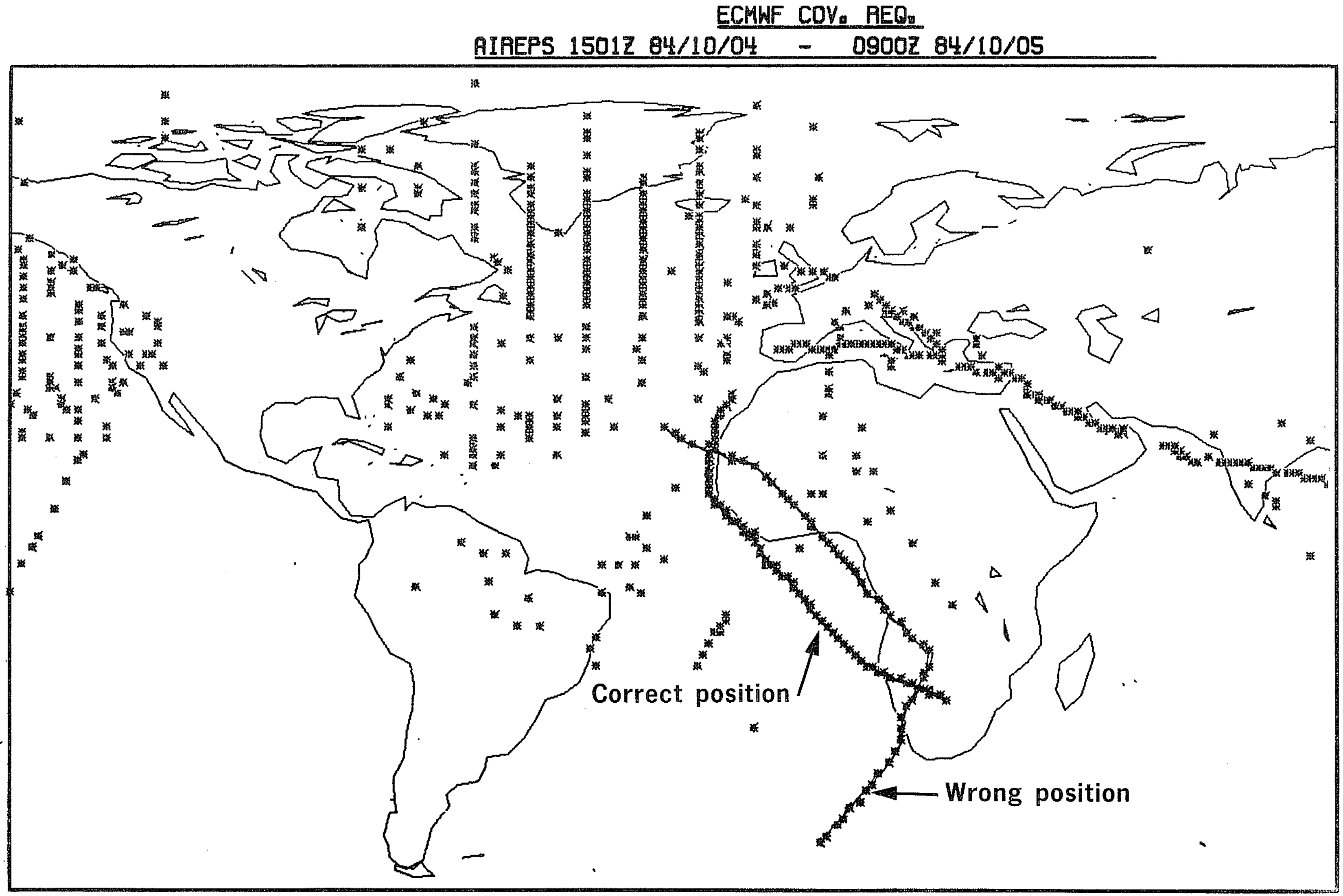

Fig. 7 Example of wrong position of Aircraft report

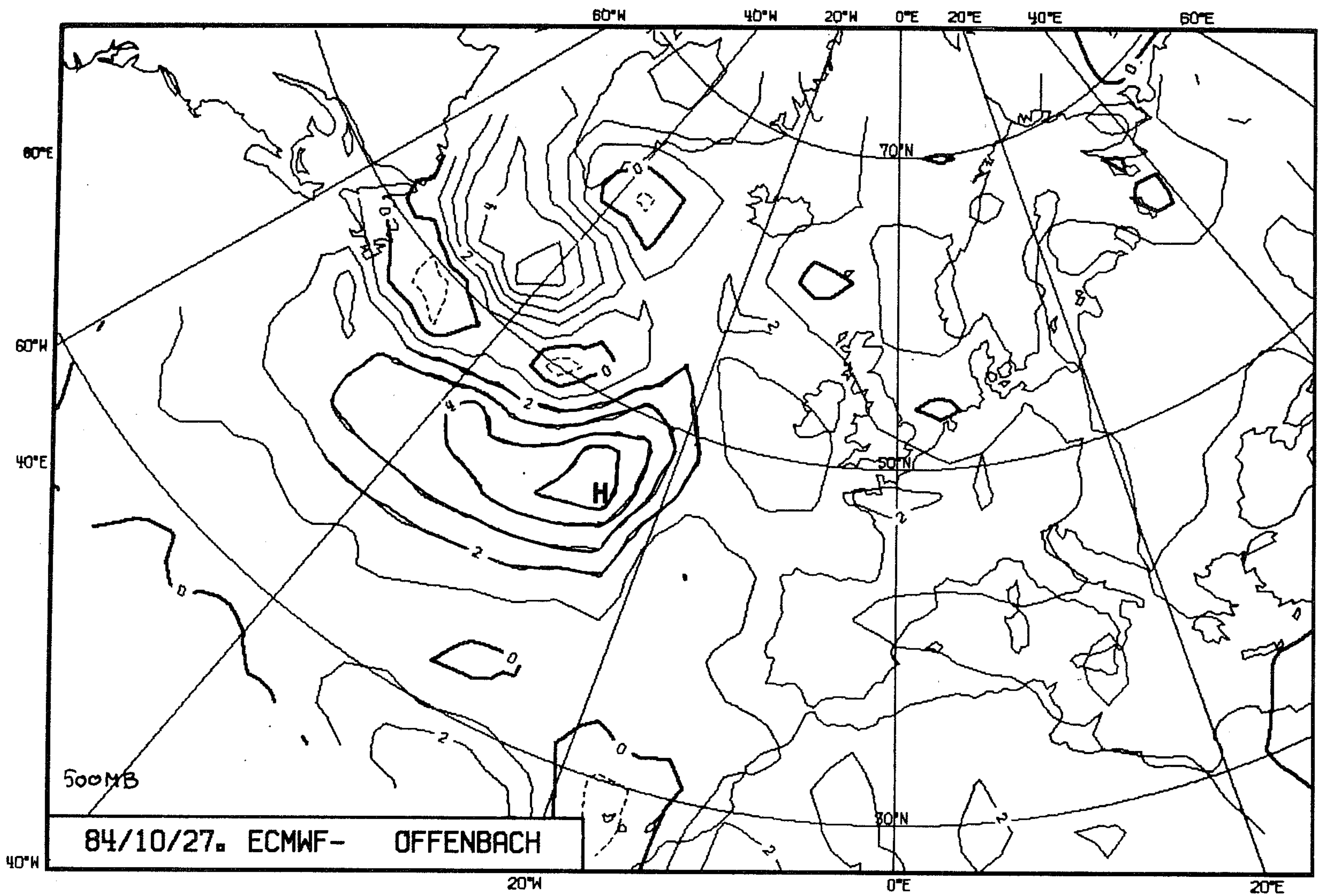

Fig. 8 500 mb analysis difference in decameter

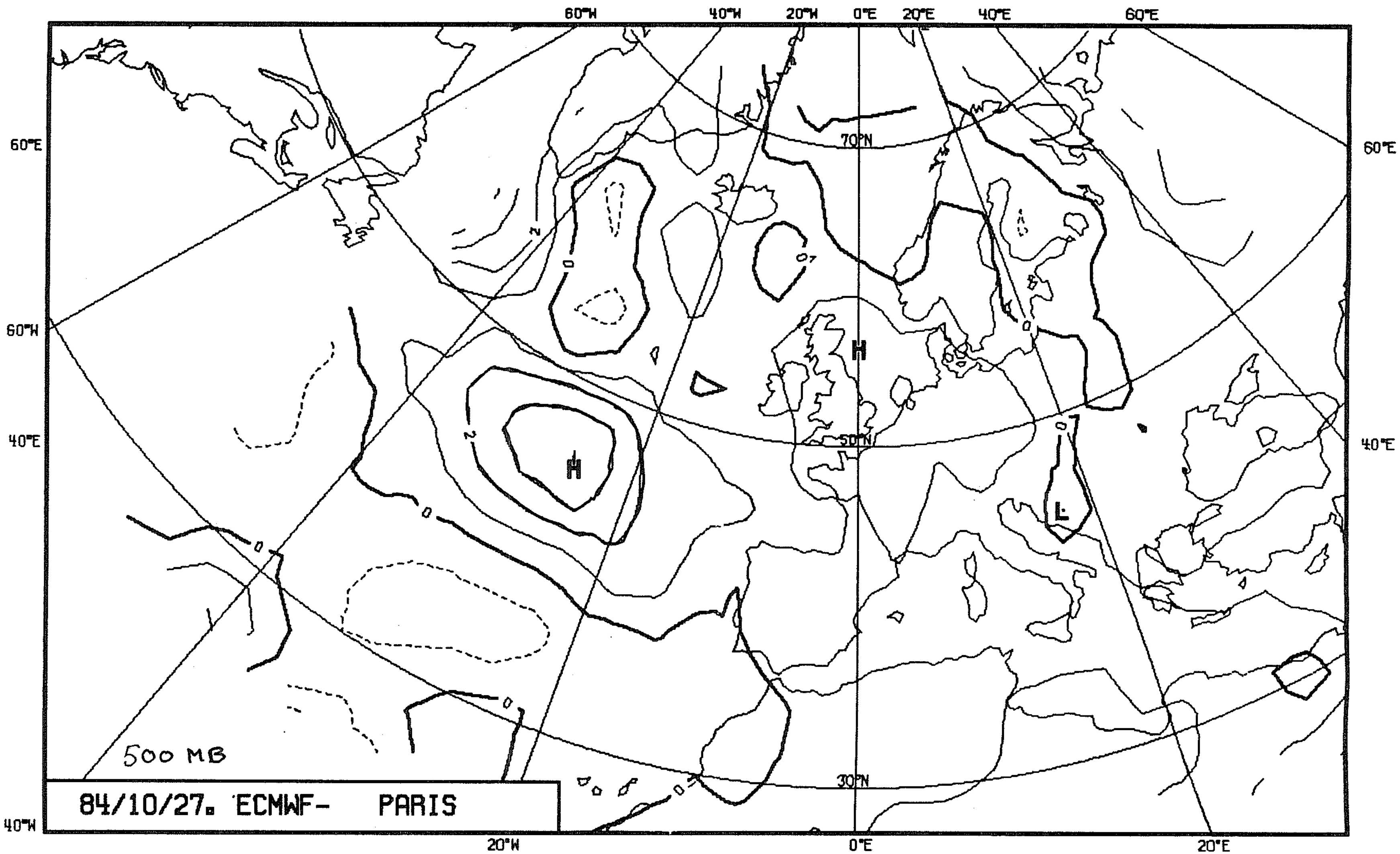

Fig. 9 500 mb analysis difference in decameter

Fig. 10: 12z AIREP reports received within 24 h, March 1984

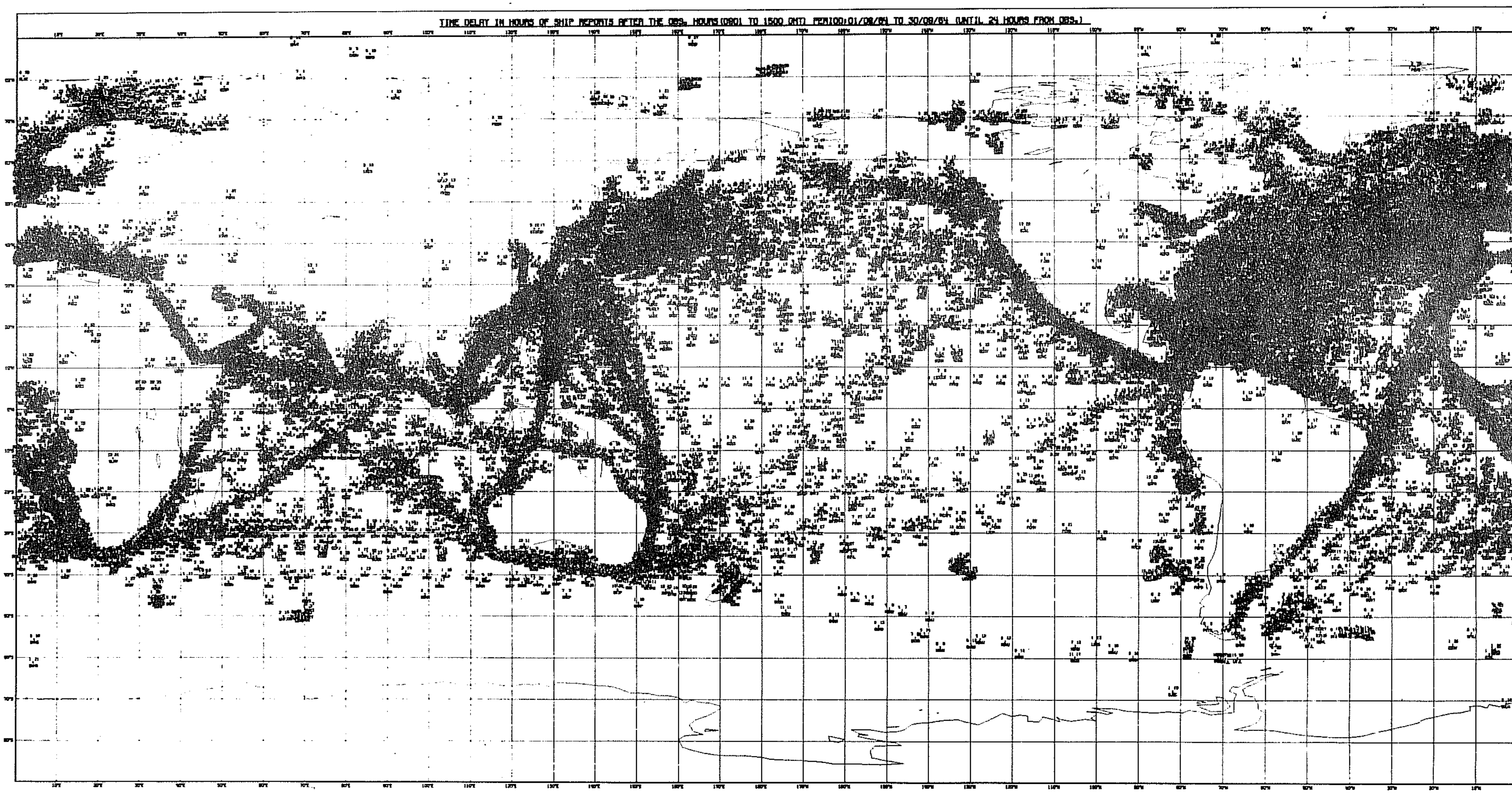

Fig. 11 12Z SHIP reports received within 24h September 1984

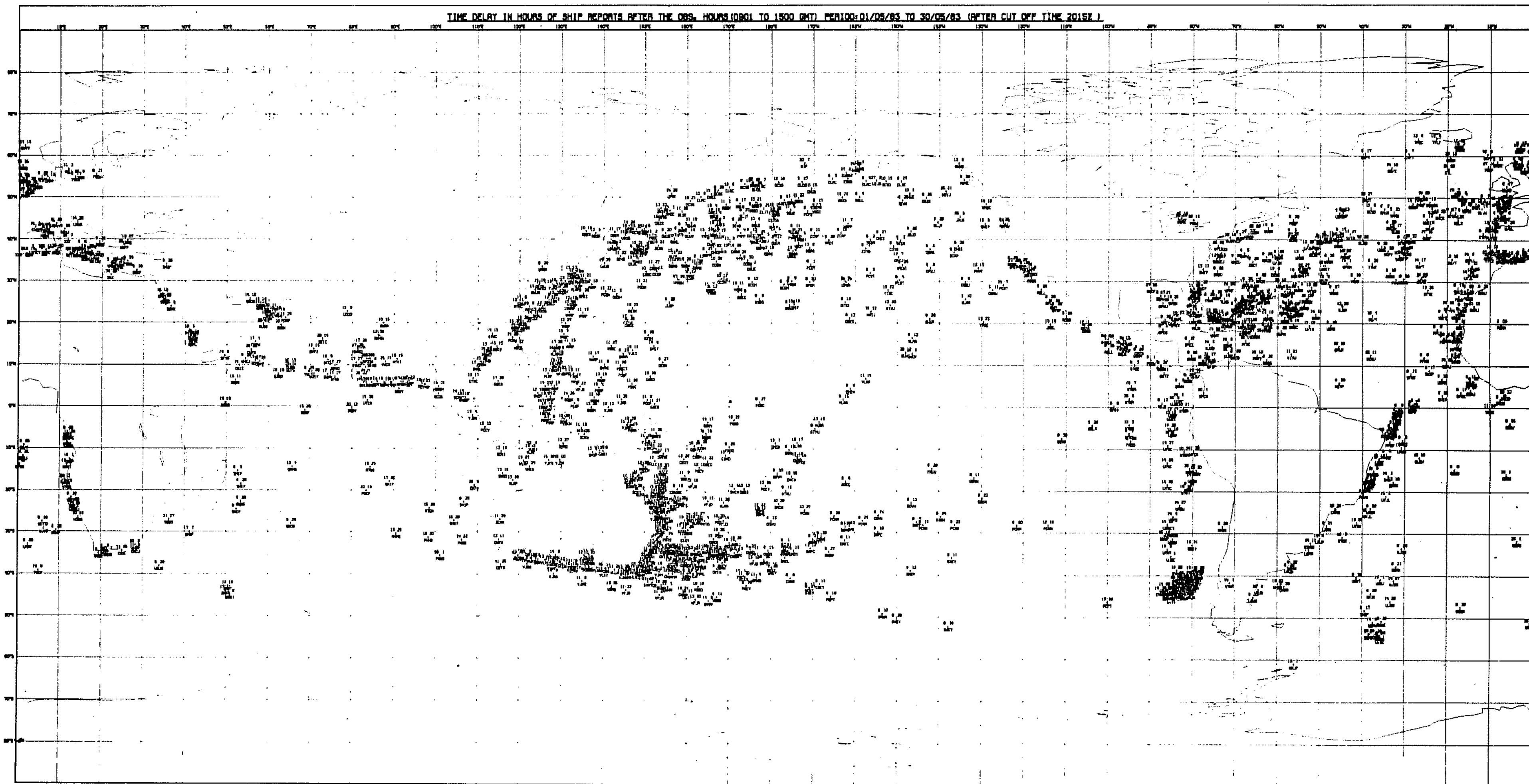

Fig. 12 12Z SHIP reports received after 2015Z cut off time May 1983

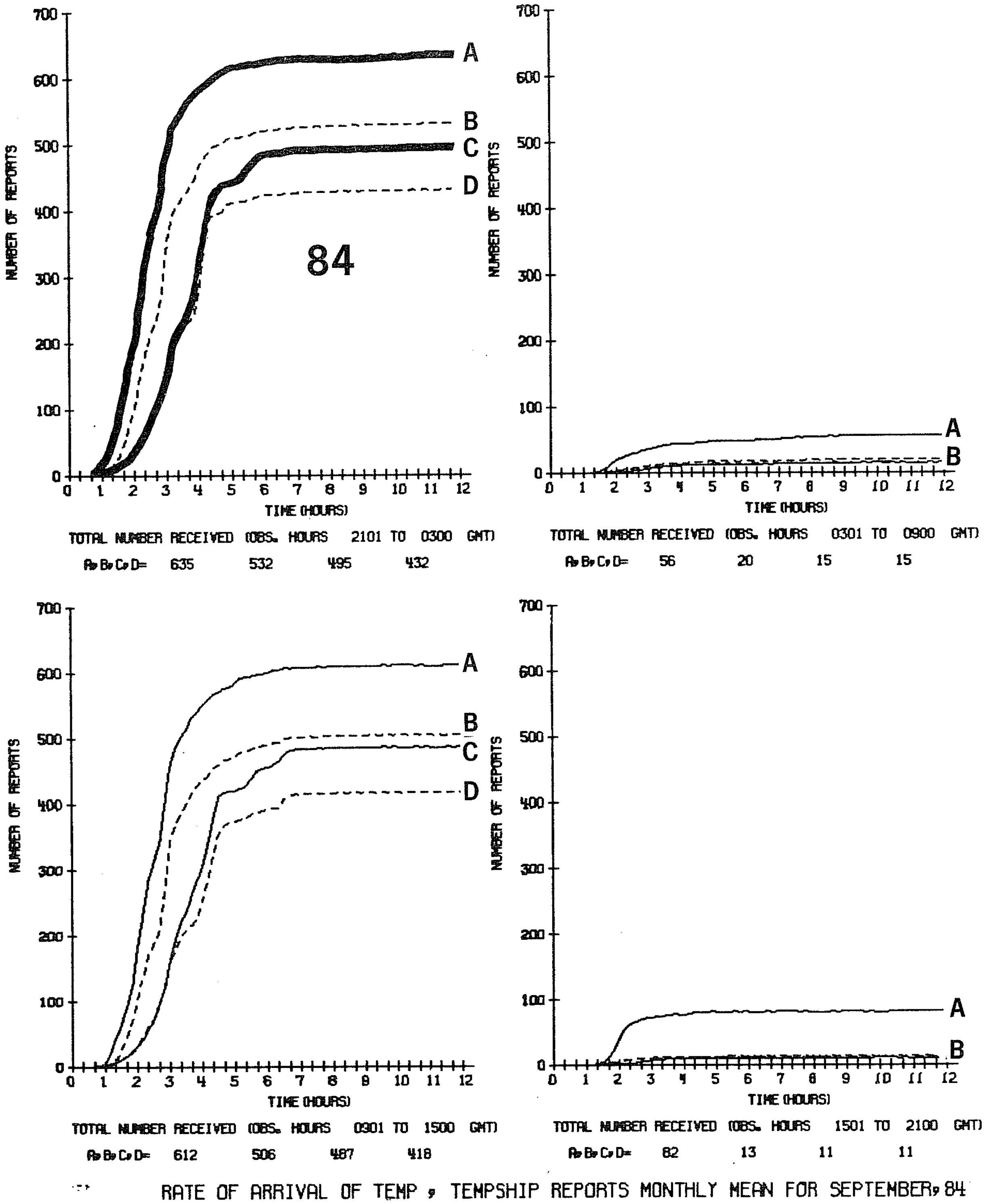

Fig. 13 Monthly mean of rate of arrival for TEMP

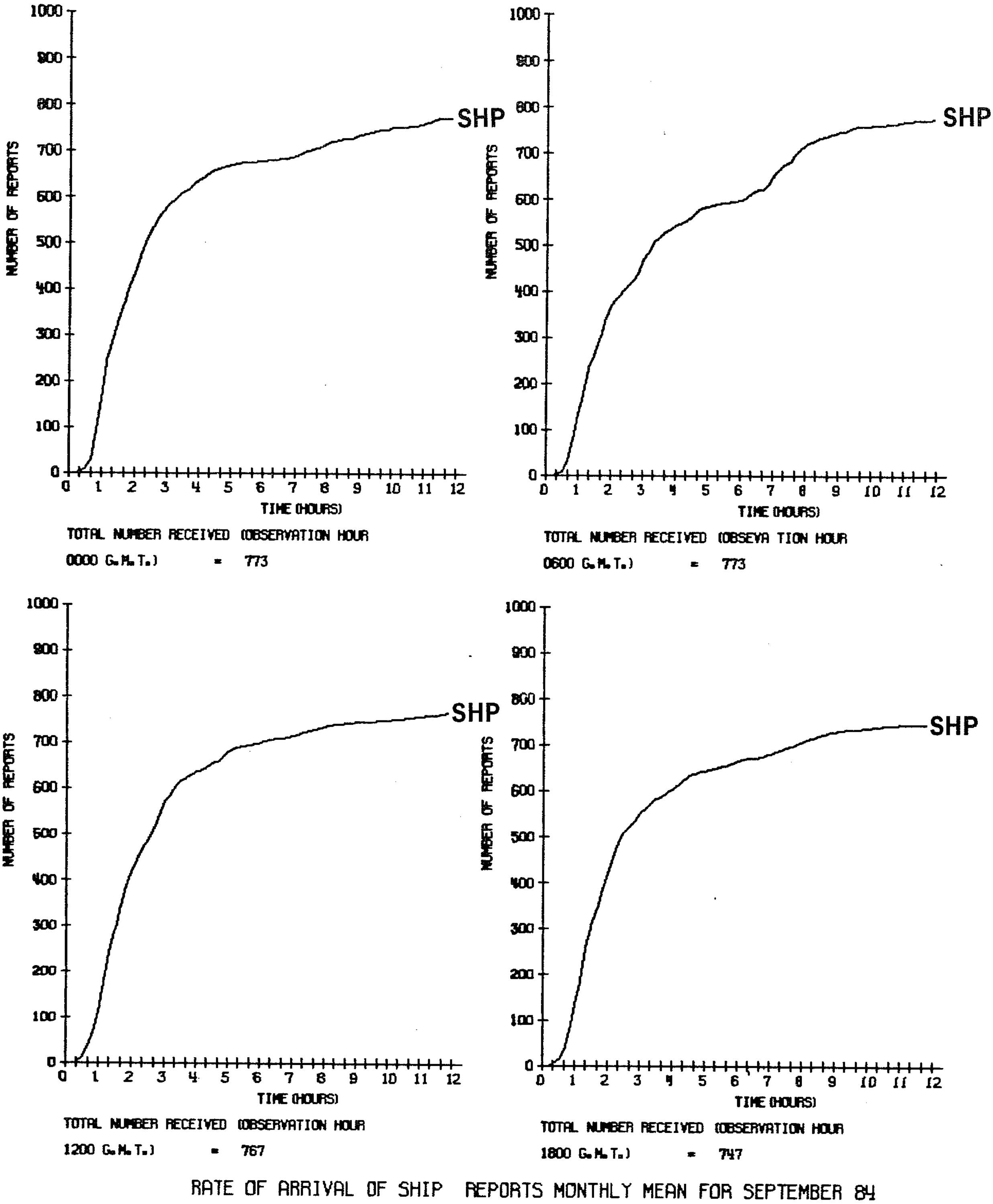

Fig. 14 Monthly mean of rate of arrival for SHIP

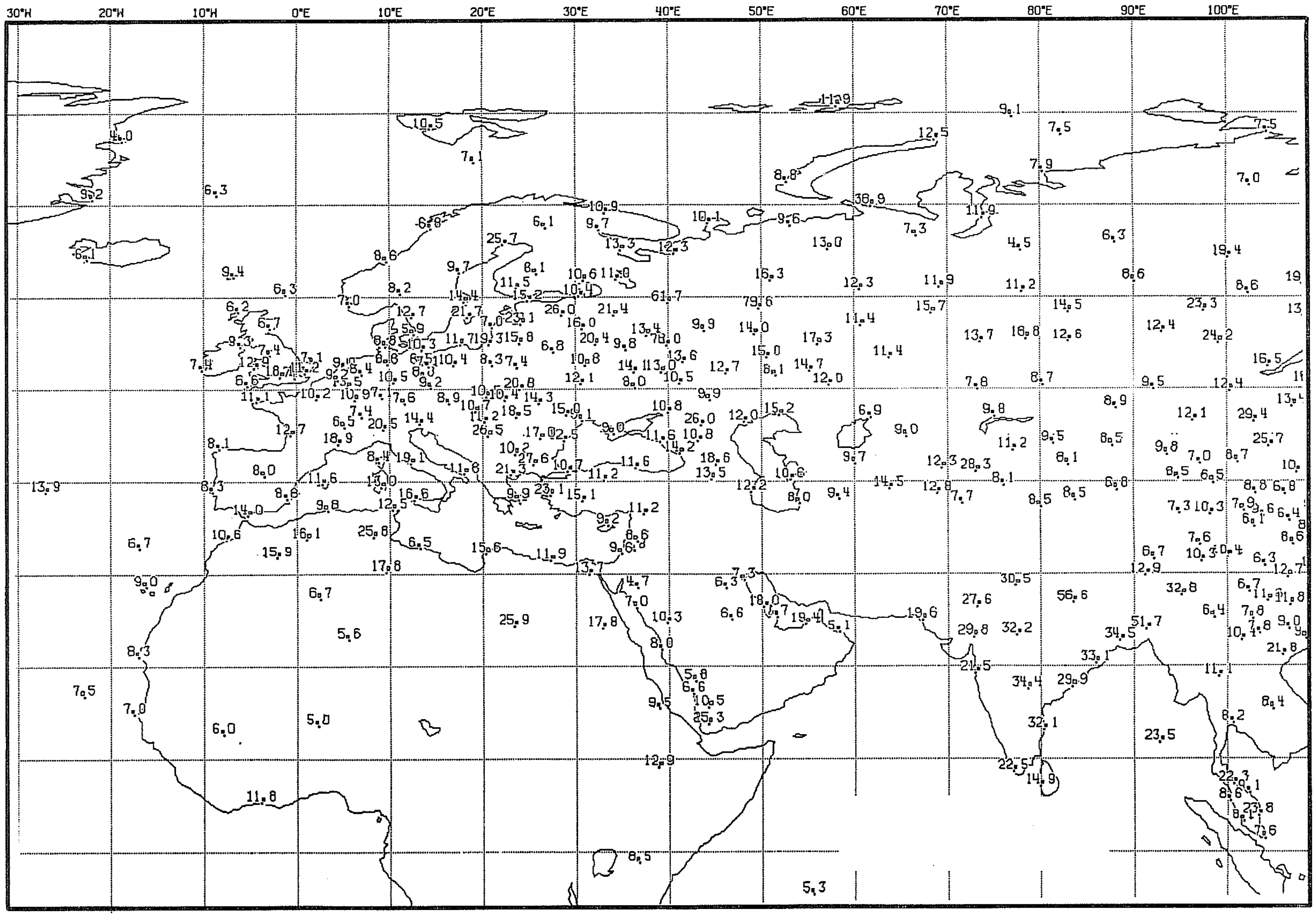

Fig. 15 Example of 500 mb height STD OBS - analysis in Meters

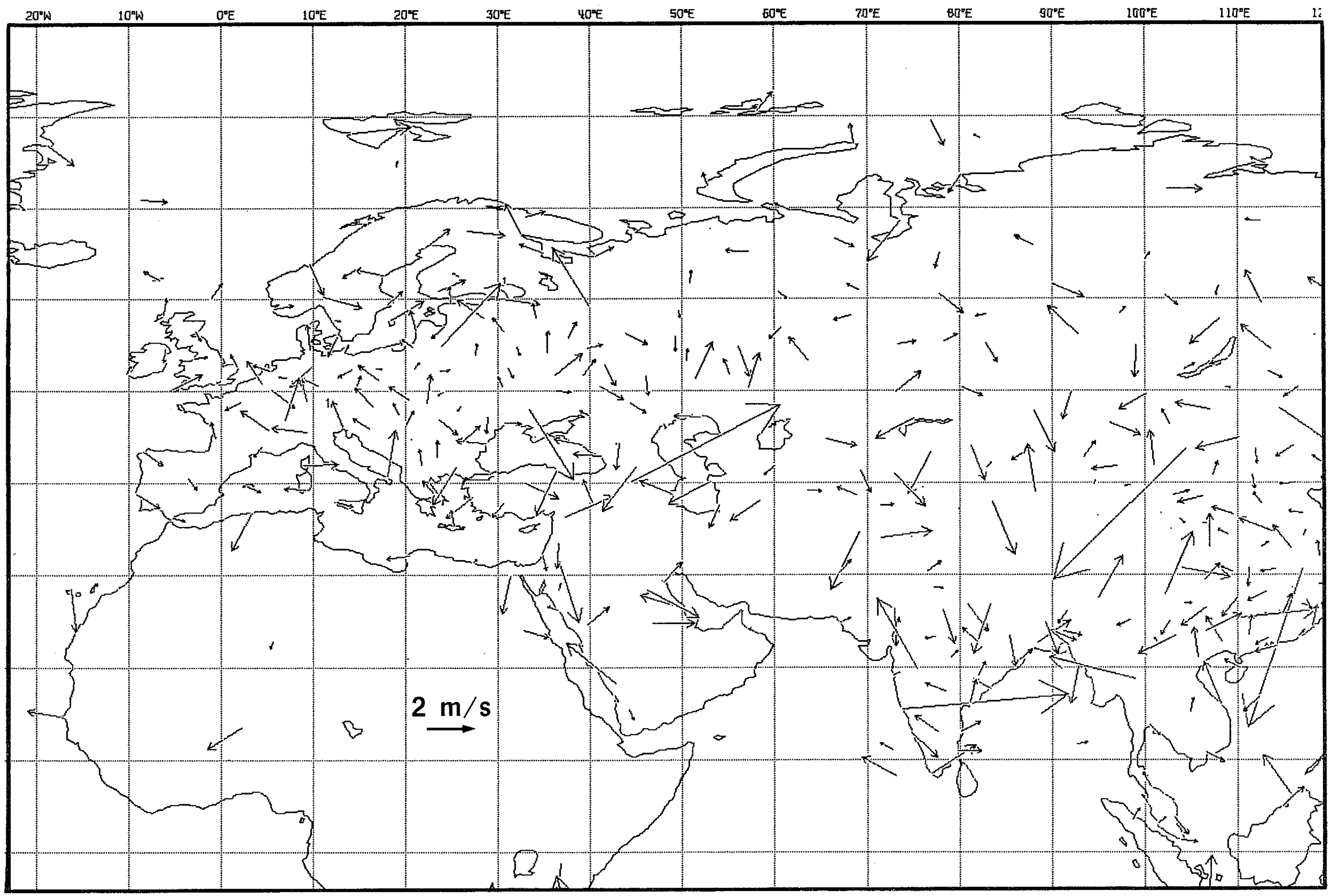

Fig. 16 Example of 700 mb wind bias

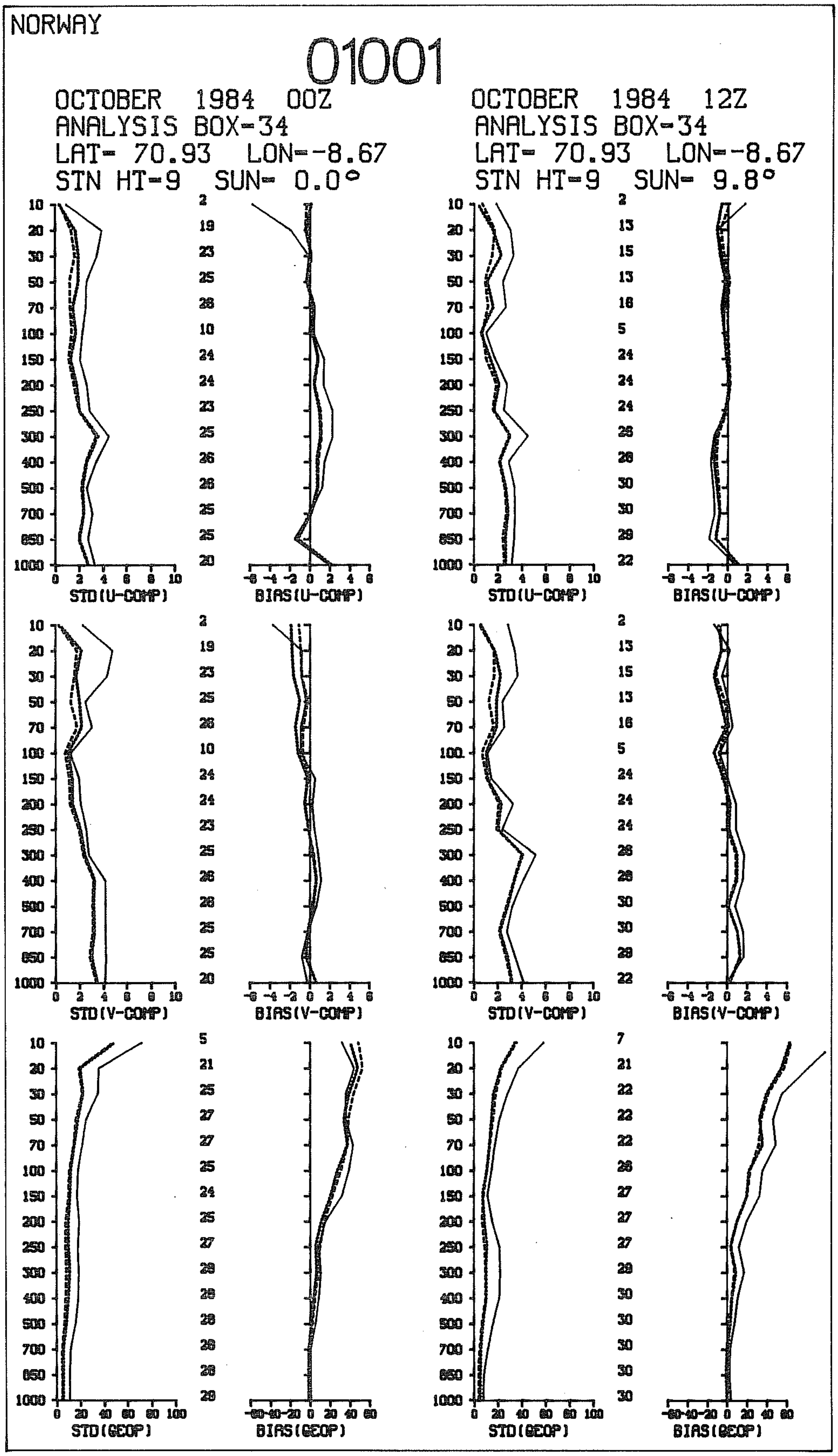

Fig. 17 Vertical mean profile of rawinsonde departure to first guess and analysis

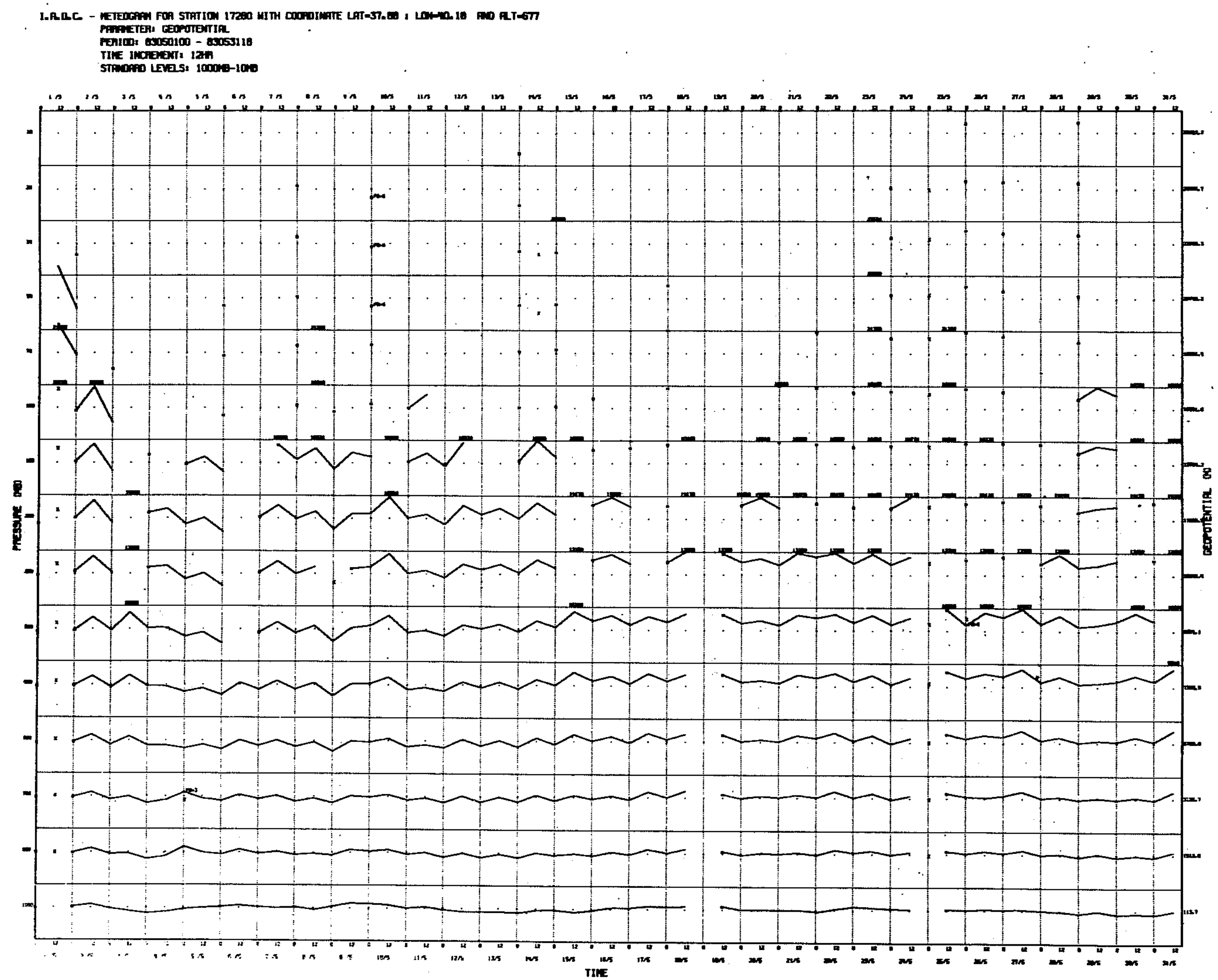

Fig. 18 Time series of geopotential height TEMP

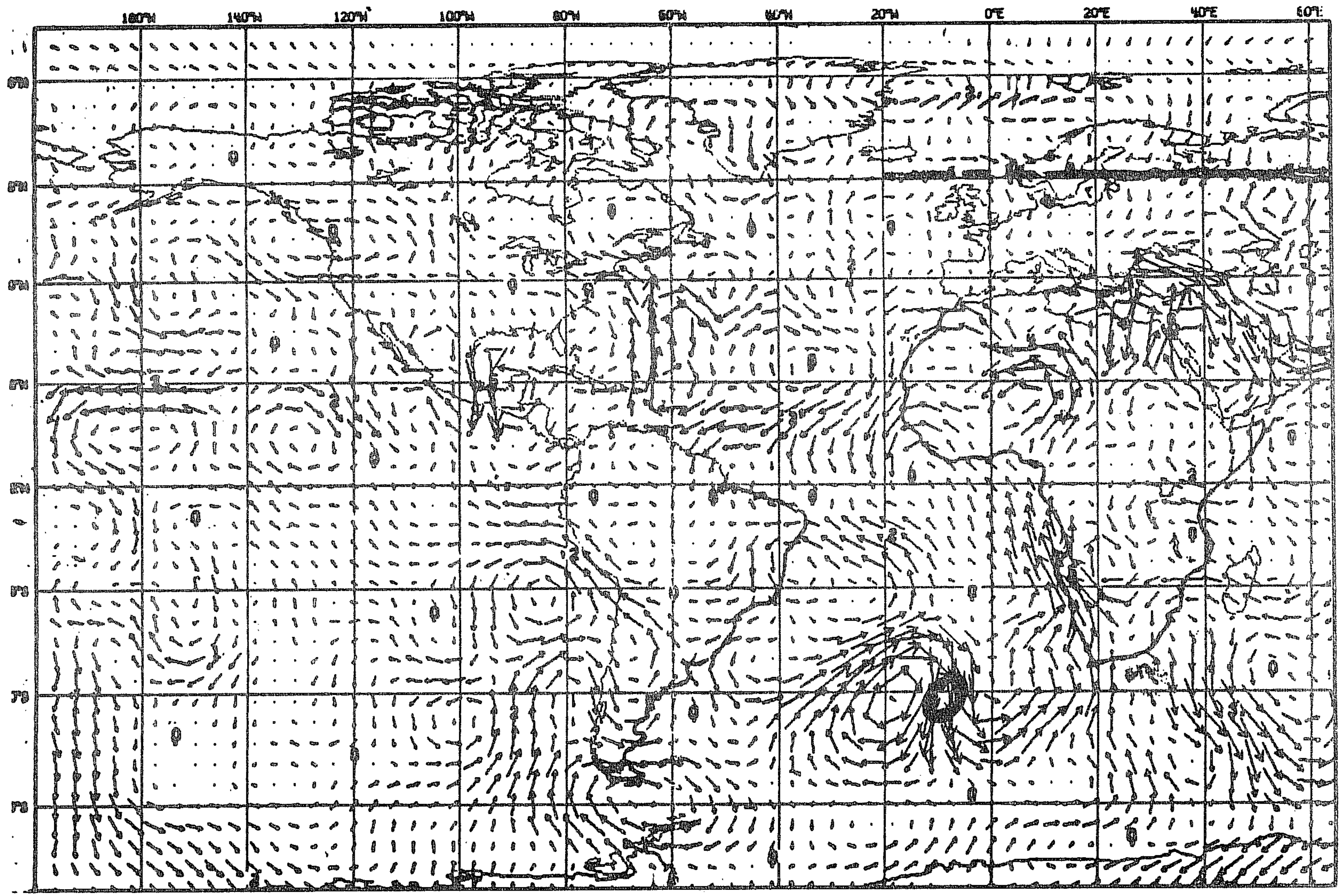

Fig. 19: 200 mb Mean wind increment, March 1984

ECMWF - DEPARTURES FOR STATION 68906 WITH COORDINATE LAT=-40.35 ; LON=-9.88 AND ALT=54 M
PARAMETER: WIND DEPARTURES FROM FIRST GUESS
PERIOD: 84030100 - 84031412
TIME INCREMENT: 24HR
STANDARD LEVELS: 1000MB-10MB

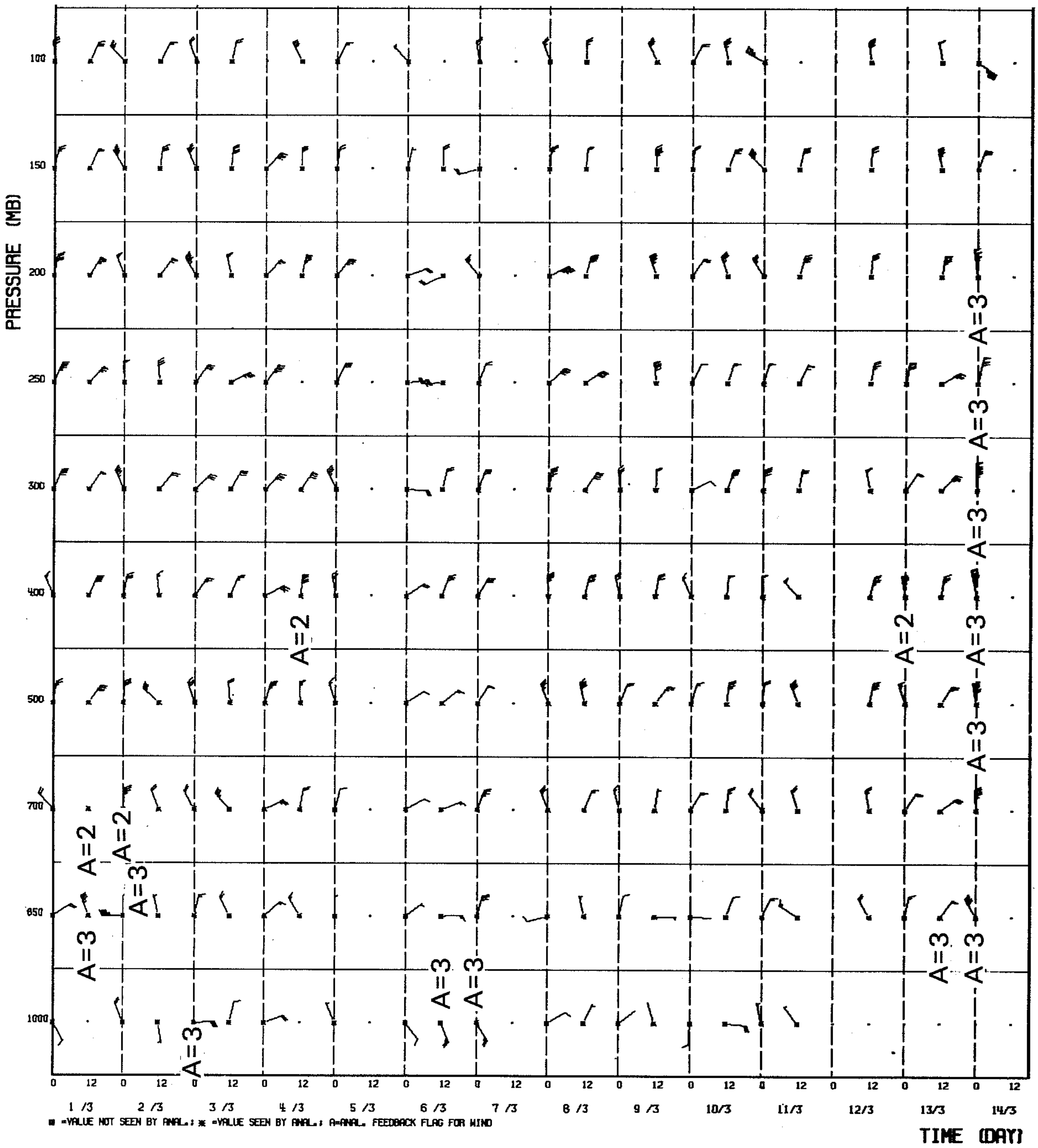

Fig. 20 Time series of wind departure from first guess

SHIP Blacklist September 1984

CALL SIGN	NO.OF OBS.	MEAN ERROR	RMS ERROR	NO.ACCEPT
UFSF	5.	13.86	13.90	0.
USV?	24.	10.13	10.73	0.
CG224	7.	10.70	10.71	0.
ELDA	8.	-9.56	9.58	0.
VCDC	14.	-9.07	9.09	0.
KSPY	14.	8.68	8.71	0.
UWYJ	7.	6.62	7.33	0.
EKRB	10.	7.07	7.29	0.
EVBC	9.	7.05	7.28	0.
ULPI	8.	6.85	6.86	0.
UWFS	5.	6.81	6.84	0.
FNPJ	24.	-6.35	6.54	0.
BOVB	11.	5.64	6.52	0.
KGPB	22.	6.04	6.11	0.
UKGJ	6.	5.97	5.99	0.
UBJA	27.	5.53	5.98	0.
OUIN	49.	5.47	5.97	0.
UOYN	6.	-0.59	5.93	0.
XPRT	24.	-3.91	5.15	0.
VCWX	18.	-4.90	5.09	0.
EWXM	19.	5.04	5.08	0.
CYLY	19.	4.88	5.00	0.
PDFT	18.	-4.84	4.91	0.
UEBV	10.	4.88	4.91	0.
EUOC	9.	-4.35	4.90	0.
ELDB8	7.	-4.53	4.57	0.
UPEX	12.	4.30	4.47	0.
EV?B	7.	-4.32	4.40	0.
S6BV	6.	4.18	4.28	0.
ESUW	5.	4.06	4.14	0.
EWGG	8.	3.77	4.04	0.
YUGX	6.	3.84	3.89	0.
HOCH	16.	-3.84	3.87	0.
UHCJ	11.	3.46	3.85	0.
ONMM	5.	3.74	3.79	0.
UQHK	5.	3.64	3.77	0.
URYH	7.	-3.69	3.77	0.
OYHI	5.	3.59	3.67	0.
VCNK	17.	-0.94	3.56	0.
UHCQ	8.	3.47	3.52	0.
HSBM	12.	-3.39	3.43	0.
VGXQ	22.	-0.61	2.39	0.
VOCD	11.	0.03	0.61	0.
VXGS	20.	0.14	0.59	0.

Fig. 21 Ship blacklist

OOZ 0984 NUMBER OF OBS 200-250MB

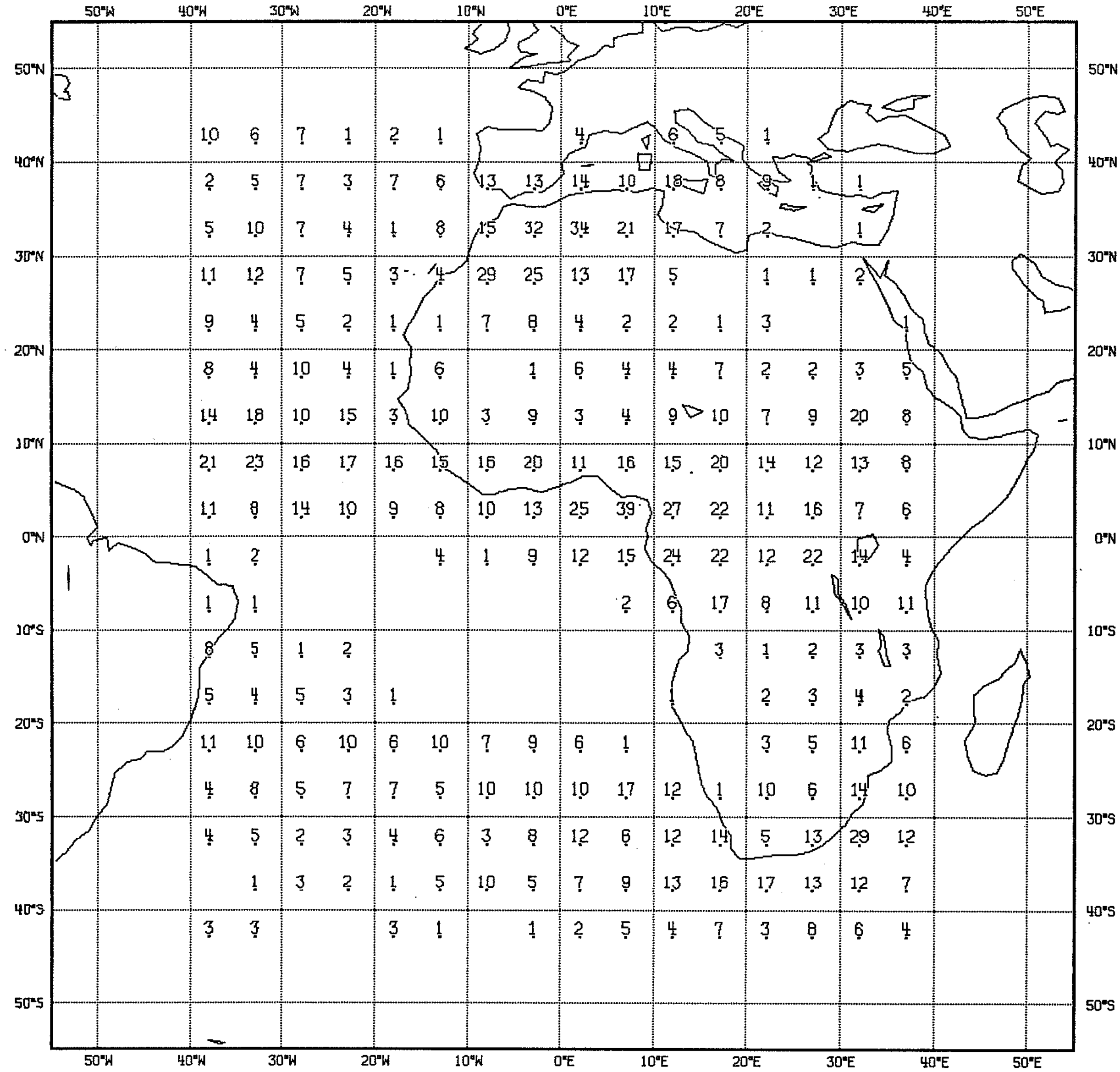

Fig. 22 Number of SATOB winds September 1984

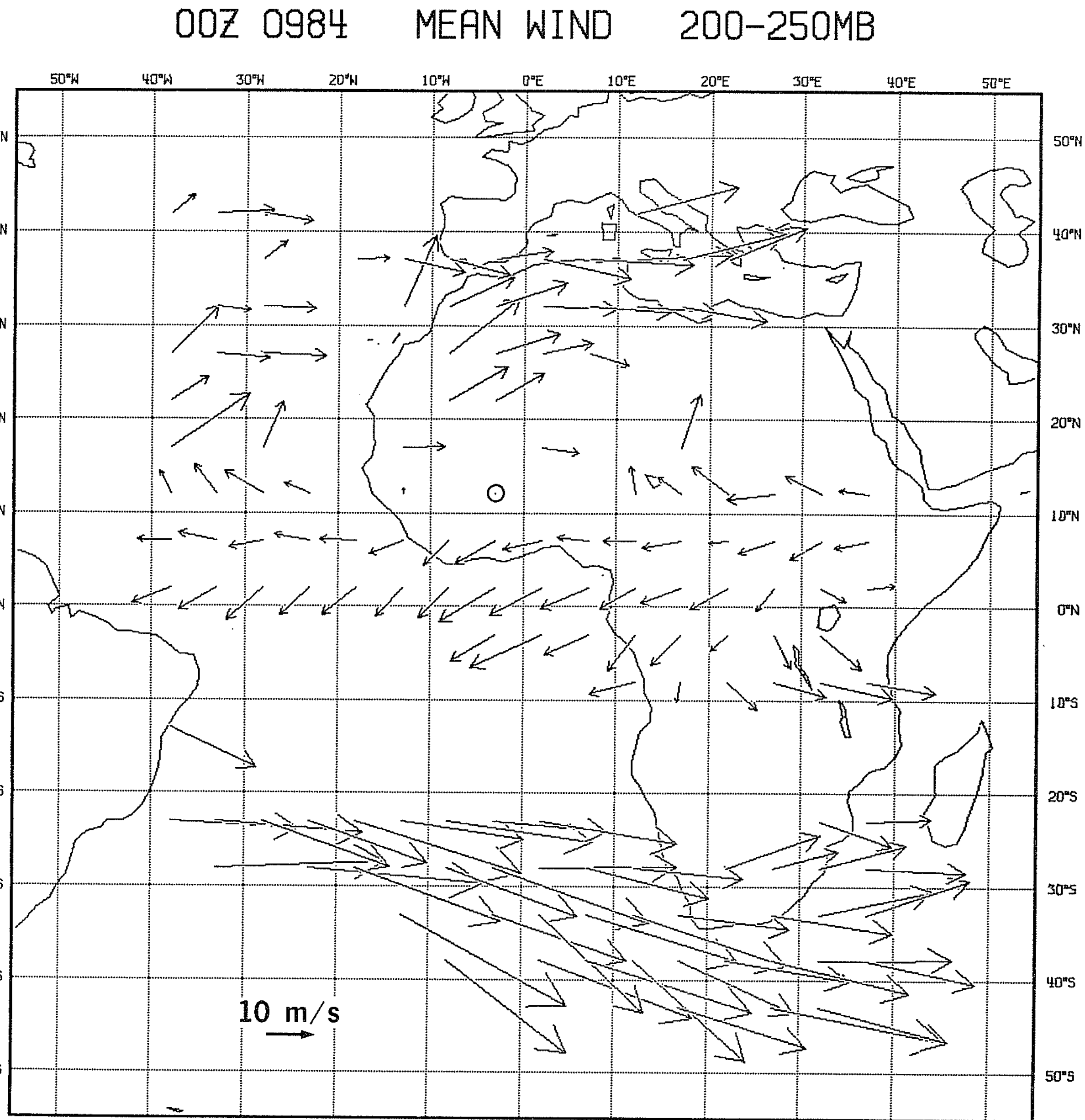

Fig. 23 Mean SATOB observed wind September 1984

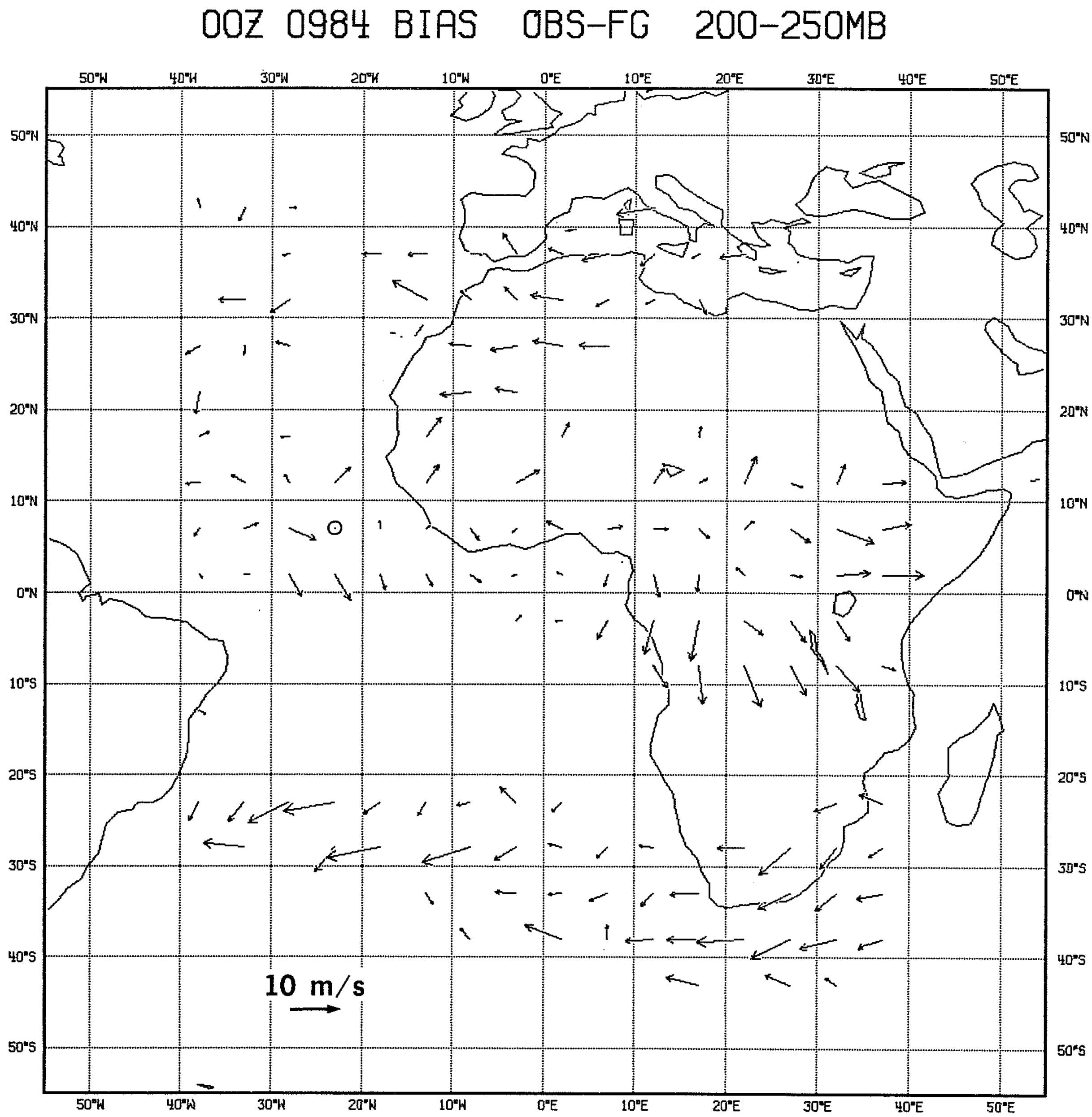

Fig. 24 SATOB bias September 1984

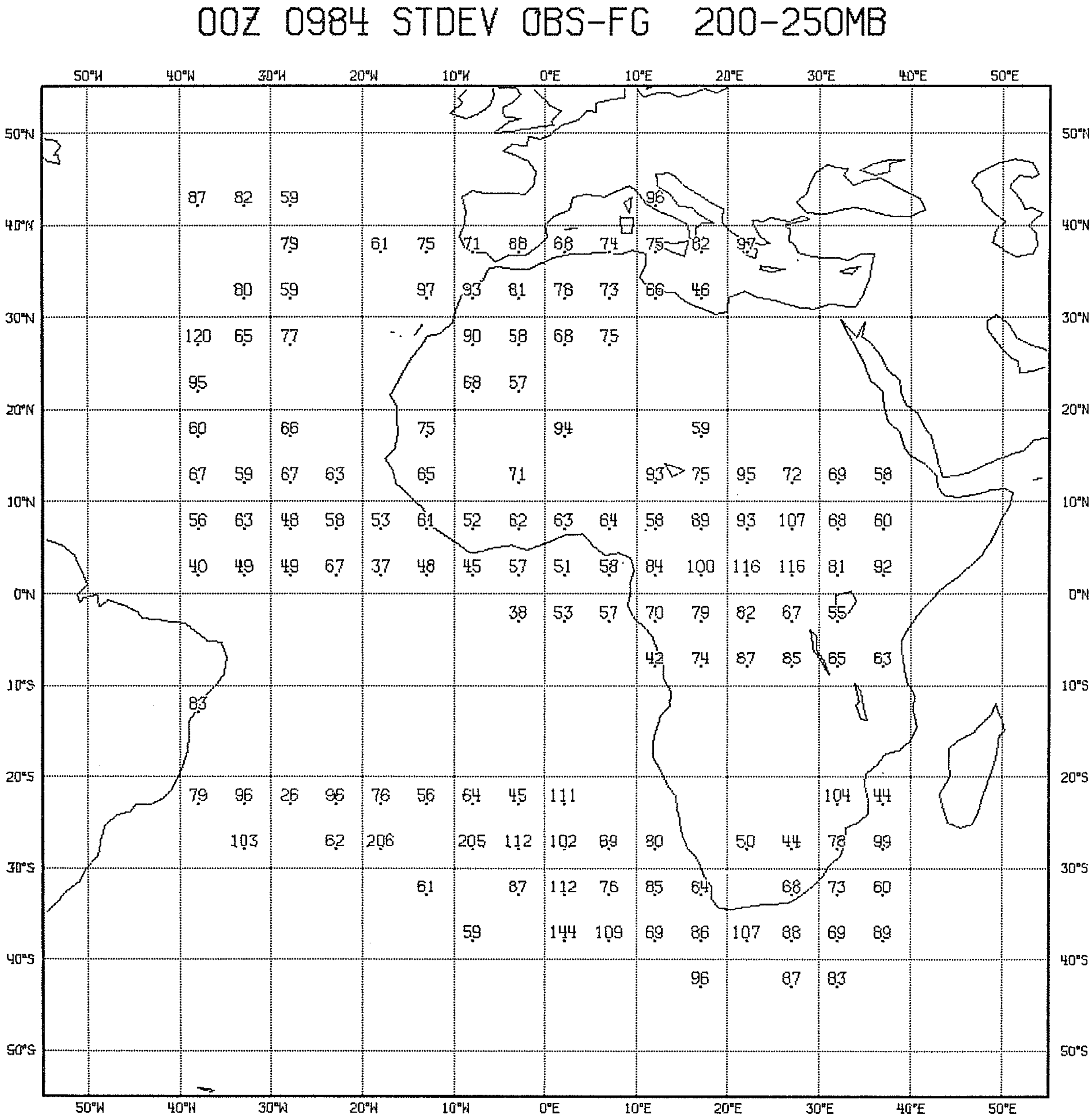

Fig. 25 SATOB standard deviation OBS-FG in 1/10 meter September 1984

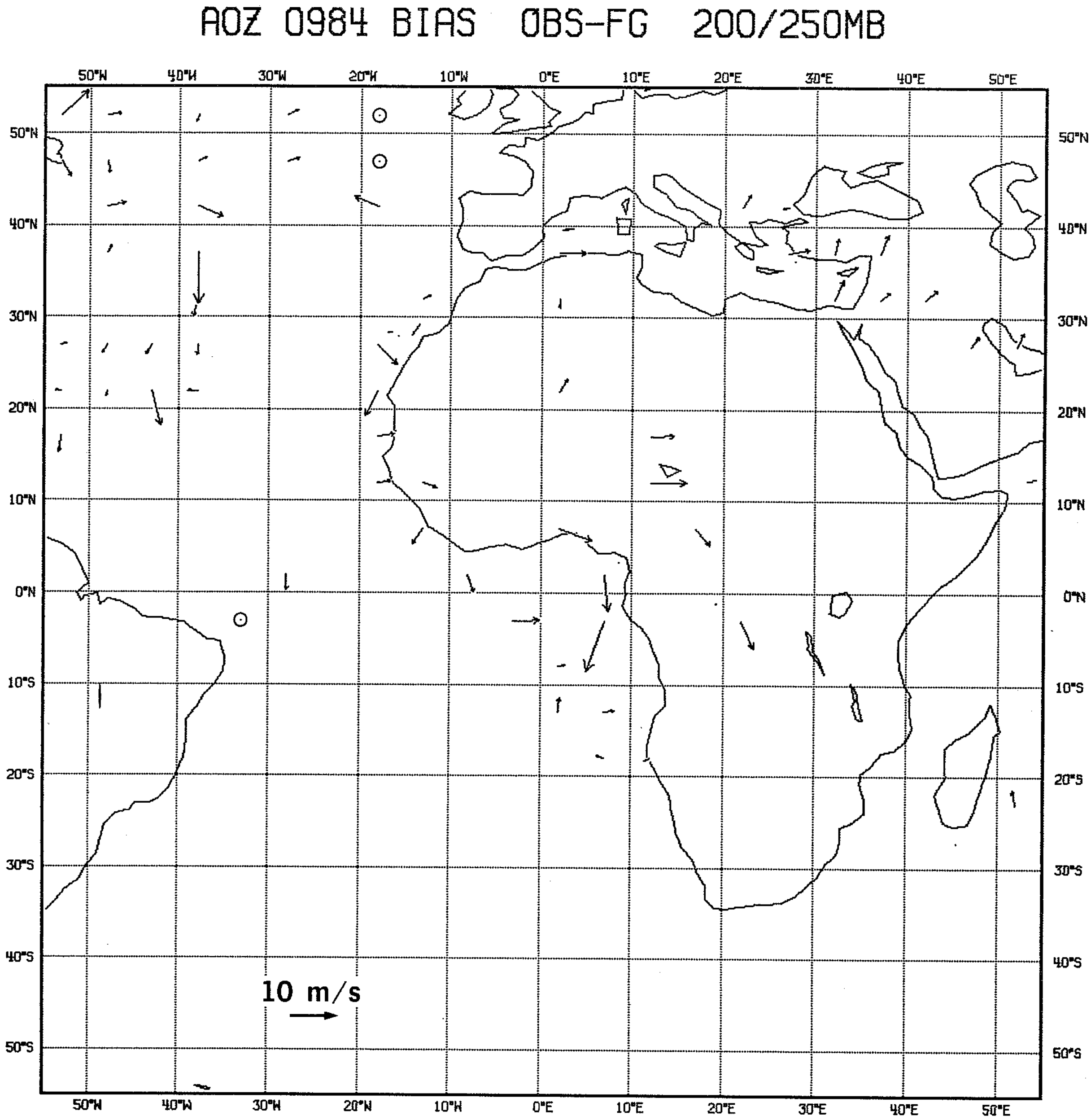

Fig. 26 AIREP bias September 1984

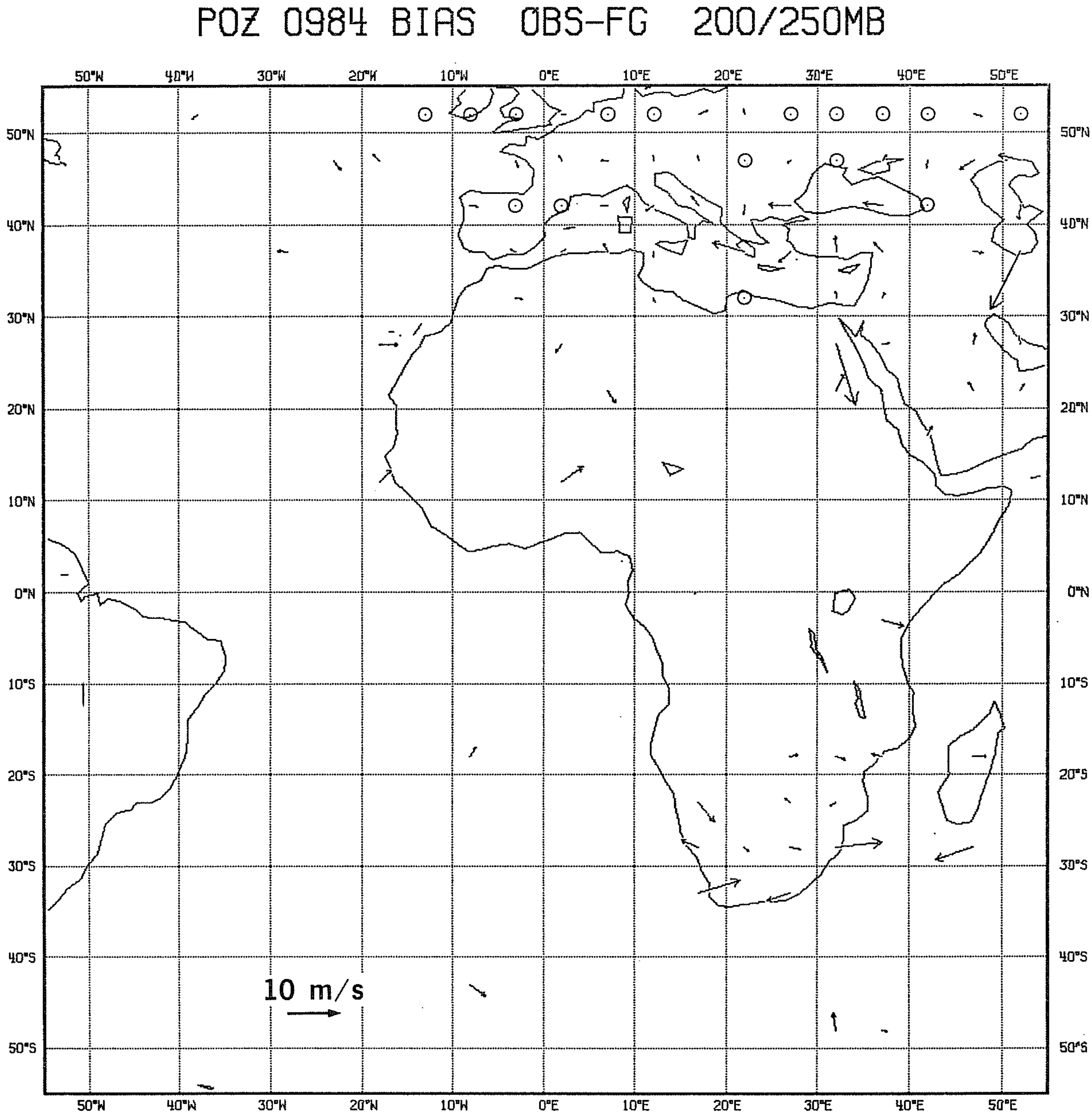

Fig. 27 PILOT and TEMP bias September 1984

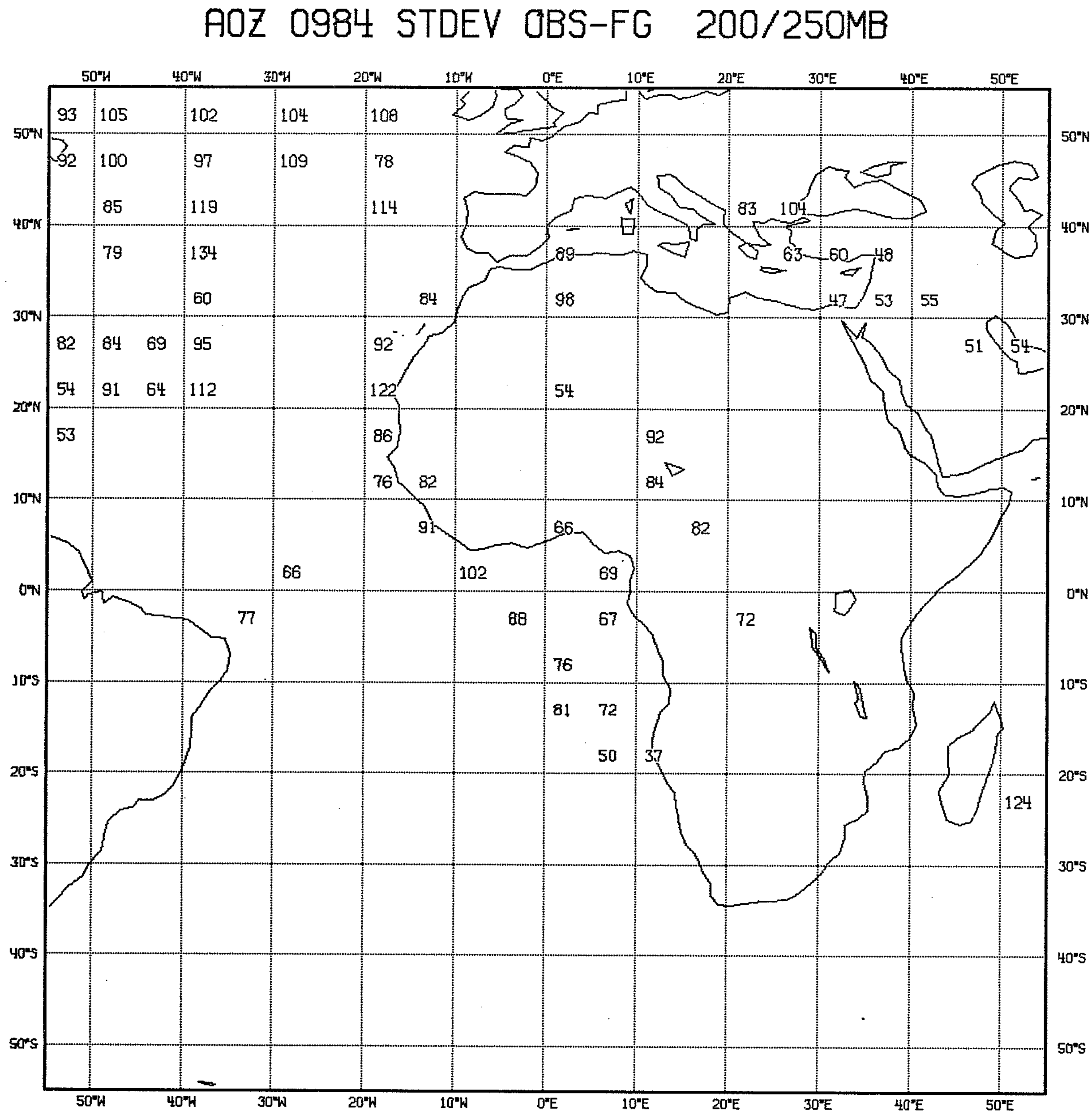

Fig. 28 AIREP standard deviation OBS-FG in 1/10 meter September 1984

POZ 0984 STDEV OBS-FG 200/250MB

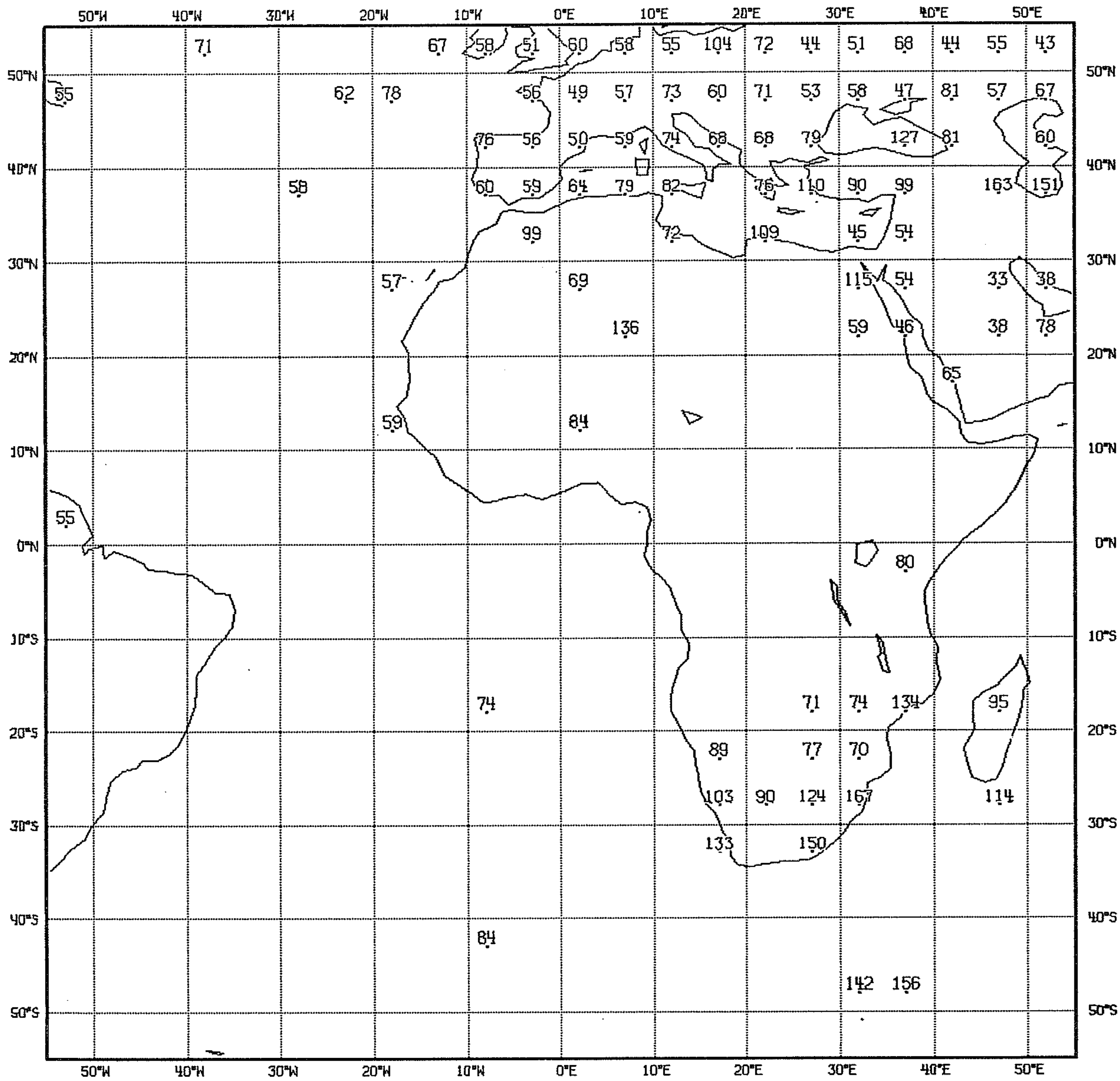

Fig. 29 PILOT and TEMP standard deviation OBS-FG in 1/10 meter
September 1984